論文 / 著書情報
Article / Book Information

題目(和文)	ファージΦMR003の宿主認識機構と黄色ブドウ球菌制御への応用
Title(English)	Host-recognition mechanism of phage ϕMR003 and its application to controlling of Staphylococcus aureus
著者(和文)	PENGChanthol
Author(English)	Chanthol Peng
出典(和文)	学位:博士(工学), 学位授与機関:東京工業大学, 報告番号:甲第11296号, 授与年月日:2019年9月20日, 学位の種別:課程博士, 審査員:丹治 保典,和地 正明,福居 俊昭,蒲池 利章,小倉 俊一郎
Citation(English)	Degree:Doctor (Engineering), Conferring organization: Tokyo Institute of Technology, Report number:甲第11296号, Conferred date:2019/9/20, Degree Type:Course doctor, Examiner:,,,,
学位種別(和文)	博士論文
Type(English)	Doctoral Thesis

Host-recognition mechanism of phage ϕMR003 and its application to controlling of *Staphylococcus aureus*

Doctoral Thesis by PENG Chanthol

2019

Department of Life Science and Technology

School of Life Science and Technology

Tokyo Institute of Technology

Academic Supervisor: Professor Yasunori TANJI

1 Table of Contents

List of Table

List of Figure

List of abbreviation

aux: auxiliary gene

CA-MRSA: Community-associated methicillin-resistant *Staphylococcus aureus*

CAMHB: Cation adjusted mueller hinton broth

CFU: Colonies forming unit

CLSI: Clinical laboratory standard institute

EOP: Efficiency of plating

fem: factor essential for methicillin resistance gene

GlcNAc: *N*-acetylglucosamine

GroP: Glycerolphosphate

HA-MRSA: Healthcare-associated methicillin-resistant *Staphylococcus aureus*

ICTV: International committee on taxonomy of viruses

LA-MRSA: Livestock-associated methicillin-resistant *Staphylococcus aureus*

ManNAc: *N*-acetylmannosamine

MIC: Minimum inhibitory concentration

MRSA: Methicillin-resistant *Staphylococcus aureus*

OD_{660}: Optical density at 660 nm

ORF: Open reading frame

PBPs: Penicillin binding proteins

POT: Phage open reading frame

PVL: Panton-valentine leucocidin

RboP: Ribitol phosphate

RBPs: Receptor binding proteins

SCC*mec:* Staphylococcal cassette chromosome *mec*

TEM: Transmission electron microscopy

VALs: Virion-associated lysin

VAPGHs: Virion-associated peptidoglycan hydrolases

WTA: Wall teichoic acid

CHAPTER 1 General Introduction

1.1 An overview of *Staphylococcus aureus*

Staphylococcus aureus is a Gram-positive bacterium, appears in a spherical shape and is commonly in clusters similar to a bunch of grapes when observed under the light microscope. The name 'Staphylococcus' was derived from Greek, meaning a bunch of grapes (staphyle) and berry (kokkos). While the term 'aureus' which is derived from Latin, refers to the color of gold. The diameter of the cells ranges from 0.5 to 1.0 μm. *S. aureus* forms fairly large yellow or white colonies on nutrient rich agar media. The yellow color of the colonies is known by carotenoids produced by the cell (Gnanamani et al. 2017). *S. aureus* causes various infectious diseases such as skin infections, bacteremia, pneumonia, food poisoning and so on. The ability of *S. aureus* to become resistant to multiple classes of antibiotics is a challenge in its infectious disease treatment (Gnanamani et al. 2017). The World Health Organization has declared the accelerated development of antibiotic-resistant bacteria as one of the top ten threats to public health (WHO 2019).

1.2 Methicillin-resistant *Staphylococcus aureus*

S. aureus strains that are resistant to methicillin or oxacillin are called methicillin-resistant *S. aureus* (MRSA). MRSA is a major human pathogen and multi-drug resistant bacterium widely found in healthcare and community settings worldwide (WHO 2014).

Healthcare-associated (HA) MRSA often infects patients in intensive care units or patients who have stayed for a long period in hospitals. HA-MRSA can cause various infections including bloodstream infections, respiratory tract infections, urinary tract infections, and surgical-wounds and device-associated infections (Doulgeraki et al. 2017; Papadopoulos et al. 2018). In Japan, MRSA has been identified at high level (40–70%) in healthcare settings which is critical to infection treatment (Shigemura et al. 2005; Kunishima et al. 2010). HA-MRSA strains such as New York/Japan clone have been dominantly isolated in Japan. However, the number of community-associated (CA) MRSA clones is increasing and the ratio of these clones is more than 50% (Harada et al. 2018).

CA-MRSA causes skin and soft tissue infection in healthy people and those who have had no recent healthcare exposure. CA-MRSA has been reported to be more pathogenic than HA-MRSA due to the production of a cytotoxin known as Panton-Valentine leukocidin (PVL) (Doulgeraki et al. 2017; Papadopoulos et al. 2018). Approximately 97% of MRSA isolates from

skin and soft tissue infection were identified as USA300 (CA-MRSA), and about 98% harbored staphylococcal cassette chromosome *mec* (SCC*mec*) type IV, with isolates from emergency clinics testing positive for PVL toxin (Moran et al. 2006). MRSA infections that are prevalent in Europe, Africa, and other countries in the Asia-Pacific region are of great concern as well (Lee et al. 2018).

Besides from HA-MRSA and CA-MRSA, the emergence of livestock-associated (LA) MRSA has provoked a great concern in food-producing animals and associated foodstuff. Food and animal are vectors of transmission of the MRSA strains (Leone et al. 2010; Doulgeraki et al. 2017). Many reports have identified the presence of MRSA in different retailed meat products include raw meat and dairy products (milk and cheese) (Kamal et al. 2013; Doulgeraki et al. 2017). In some cases, the MRSA isolates are identified as HA-MRSA or CA-MRSA, indicating that food handlers are likely to be the source of the bacteria. In other surveys, LA-MRSA strains are the primary isolates, indicating an animal source of contamination. LA-MRSA has been isolated from both human and animal infections, as well as from bovine mastitis cases. When SCC*mec* characterization is carried out with MRSA isolates of food origin, SCC*mec* III and IV are identified in isolates recovered from cows' milk and chicken. Foodborne illness causing severe symptoms due to MRSA has been documented, illustrating the potential impact of this pathogen on human health (Doulgeraki et al. 2017).

1.3 Mode of action and resistant mechanism to β-lactam antibiotic in *S. aureus*

The antibiotic-resistant development is a threat to public health. The treatment of staphylococcal infection has been with β-lactam antibiotics. However, as the emergence of MRSA, alternative antibiotics have been used such as vancomycin, daptomycin, and linezolid (Haaber et al. 2017). In order to adapt to the antibiotic attack, *S. aureus* commonly use two different major genetic strategies such as a mutation in a gene which often linked with the antibiotic target and the acquisition of antibiotic-resistant gene through horizontal gene transfer (Foster 2017).

The major targets of antibiotics in staphylococci include the cell envelop, the ribosome and nucleic acids (Foster 2017). The *S. aureus* can develop resistant through horizontal transfer of resistance genes encoded by plasmids, transposons and the SCC*mec* gene (mobile genetic elements) or by mutations in chromosomal genes. The horizontally acquired resistance mechanism can occur via one of the following: enzymatic drug modification and inactivation, enzymatic modification of the drug binding site, drug efflux, bypass mechanisms involving the acquisition of a novel drug-resistant target, and displacement of the drug to protect the target. On

the other hand, the acquisition of resistance by mutation can result from alteration of the drug target that prevents the inhibitor from binding, multidrug resistance efflux pumps and multiple stepwise mutations that alter the structure and composition of the cell wall to reduce drug access to its target (Foster 2017).

1.3.1 Mode of action of β-lactam antibiotics

The β-lactam antibiotics inhibit bacterial growth by interfering with the bacterial cell wall synthesis (Kong et al. 2010). The cell wall is a rigid outer layer that maintains cell integrity and prevents cell lysis from high osmotic pressure. The cell wall is composed of a complex, cross-linked polymer of polysaccharides and peptides known as peptidoglycan (Entenza et al. 2005). The polysaccharides composed of amino sugar *N*-acetylglucosamine (NAG) and *N*-acetylmuramic acid (NAM). A five-amino-acid peptide (L-ala-D-glu-L-lys-D-ala-D-ala) is linked to the NAM sugar (Entenza et al. 2005) (Fig. 1-1a).

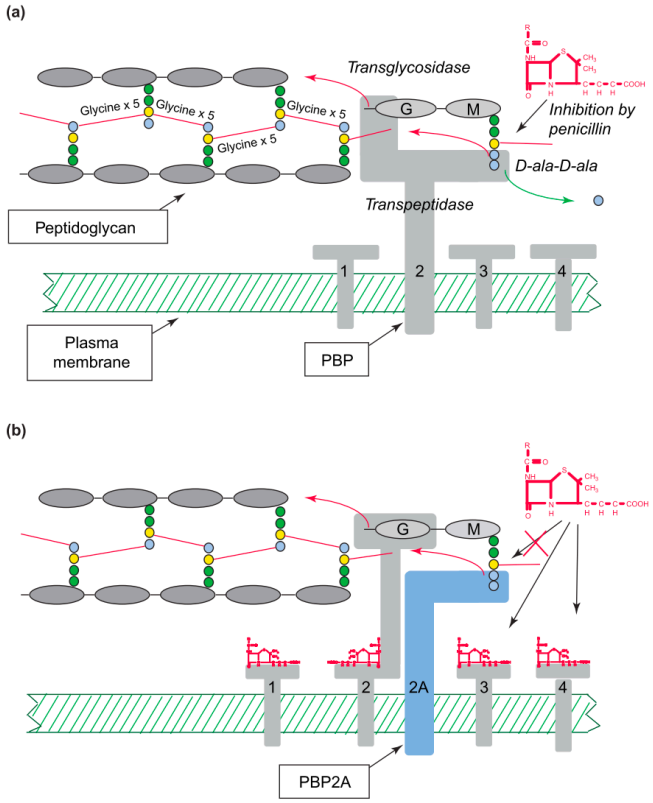

Figure 1-1 Peptidoglycan assembly in *S. aureus* and in MRSA. (a) Cell wall precursors consist of the disaccharide pentapeptides NAG and NAM-L-ala-D-glu-L-lys-D-ala-D-ala. (b) MRSA carry an additional PBP called PBP2A that has a low binding affinity to most β-lactam antibiotics. Colored circles represent the amino acids of the stem peptides. Green circles: L-alanine and D-isoglutamine, respectively; yellow circles: L-lysine; and blue circles: D-alanine; G: NAG; M: NAM (Entenza et al. 2005)

The enzyme called penicillin-binding proteins (PBPs) removes the terminal alanine in the process of forming a cross-link with a nearby peptide. The cross-links help the rigidity of cell wall. Several of these PBPs are bifunctional and retain both a transglycosidase and a transpeptidase activity.

The transglycosidase step links NAG to NAM in the nascent wall, and a transpeptidase step links the penultimate D-ala to a glycine acceptor in the nascent wall. In *S. aureus*, the lysine in position 3 of the stem peptide is almost always decorated with a pentaglycine side-chain (red bars, Fig 1-1). Penicillin is in the same class to oxacillin (β-lactam), inhibits the transpeptidase domain of PBPs. *S. aureus* carries only one bifunctional PBP (PBP2) and three monofunctional transpeptidases (PBP1, 3 and 4) (Fig 1-1a).

β -lactam antibiotics covalently bind to the active site of PBPs. This binding inhibits the transpeptidation reaction and peptidoglycan synthesis, and the cell die. The exact mechanism of cell death is not completely understood, but autolysins are involved in addition to the disruption of cross-linking of the cell wall. β-lactam antibiotics kill actively growing or synthesizing cell wall cell (Entenza et al. 2005; Pinho 2008).

1.3.2 *blaZ* and *mec*A genes as the determinants of β-lactam resistance

The most common resistant mechanism of *S. aureus* to β-lactam antibiotics is mediated by β-lactamase which hydrolyzes β-lactam-susceptible compounds. β-lactamase is encoded in the *blaZ* gene which is usually carried on a plasmid. Moreover, MRSA produces a newly acquired PBP2A encoded by the *mec*A gene (is carried in mobile genetic element, SCC*mec*), which is a wall-building transpeptidase that resists blockage by β-lactam. Under the presence of β-lactam antibiotics, the normal PBPs are blocked but not PBP2A. PBP2A has only a transpeptidase domain, and must 'hijack' the transglycosidase domain of normal PBP2 to be active (Entenza et al. 2005) (Fig 1-1b). PBP2A is absolutely required for high-level β-lactam-resistance in MRSA. Blocking its activity in isolation, as in PBP2A- negative mutants restores susceptibility to β-lactam (Pinho 2008).

Although *mec*A is the principal oxacillin resistance determinant in MRSA, several additional native genes of *S. aureus* also are essential for the full expression of oxacillin resistance in MRSA. Most of these genes called *aux* (auxiliary) or *fem* (**f**actor **e**ssential for **m**ethicillin resistance). The inactivation of *fem* genes in the presence of *mecA* in MRSA results in strains with a heterogeneous profile of oxacillin resistance. For example, the majority of cells have a low resistant, while a subpopulation appears as highly resistant. The identified *fem* genes are mostly

housekeeping genes that encode putative sensory or regulatory activities, transcription factor, proteins that have a direct or indirect role in peptidoglycan metabolism or structure. The identified *fem* genes and their function in peptidoglycan metabolism include *pbp*2, *fmt*A, *vra*SR and so on (Pinho 2008).

1.4 Bacteriophage

The widespread use of antibiotics has generated selective pressures that have driven the emergence of resistant strains, and have consequently limited treatment options for MRSA infections (Enright et al. 2002). Therefore, the use of bacteriophages (phages) has been suggested as an alternative therapy (Lin et al. 2017; Moelling et al. 2018; Azam and Tanji 2019a).

The phage therapy give several advantages over antibiotic: phage can lyse not only the susceptible but also the antibiotic-resistant bacteria; phage has high host specificity so that it does not affect normal microflora; it has antibiofilm activity; if the resistance strain arises, phages mutate alongside the bacteria to effectively infect the resistant strain (Gordillo Altamirano and Barr 2019).

Phages are viruses which can infect and replicate within a bacterial host. The term "phage" refers to "bacterium eater" that was discovered over a century ago. Since their discoveries, phages were used to treat bacterial infections in the human patient. However, after the introduction of antibiotics, penicillin since 1940, the phage studies were collapsed. Nevertheless, phage therapy was not completely abandoned in Eastern Europe such as Georgia, Russia, and Poland, phage therapy steadily investigated (Gordillo Altamirano and Barr 2019).

Phage therapy is the administration of lytic phage directly to a patient in order to lyse the bacterial pathogen that causes a clinical infection (Gordillo Altamirano and Barr 2019). The phage infection pathway involves several steps: phage adsorption on the host cell surface, DNA injection into the host, DNA replication, phage particle assembly, and host lysis (lytic cycle, Fig 1-2). In comparison, the lysogenic cycle is displayed particularly by temperate phages and results in the integration of the prophage (viral genetic material) with the bacterial genome. With this process, viral genetic is ensured to replicate through the division of host without causing any fatal consequence to the host. However, because of the viral genetic material incorporated into the host, the infected host is commonly encountered phenotypic changes such as inducing the pathogenicity of the host (Sharma et al. 2017).

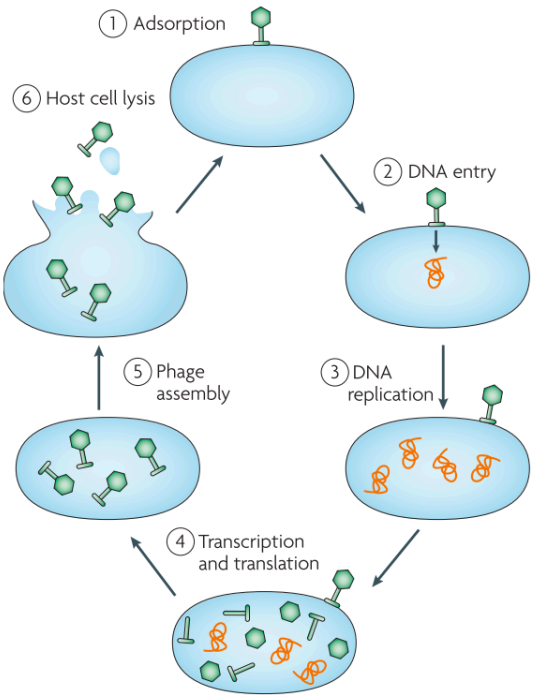

Figure 1-2 Lytic cycle of phage (Sharma et al. 2017)

1.5 Staphylococcal phage

All known *S. aureus* phages belong to order *Caudovirales* (tailed phages) which are composed of an icosahedral capsid filled with double-stranded DNA and a thin filamentous tail (Xia and Wolz 2014). Based on the tail morphology, they can be further clustered into five major families and the three most characterized include *Siphoviridae* (have a long non-contractile tail); *Myoviridae* (have a long, contractile, double-sheathed tail) and *Podoviridae* (have a very short tail) (Fig 1-3). And recently, two more families: *Ackermannviridae* and *Herelleviridae* (ICTV 2019) were added into this order.

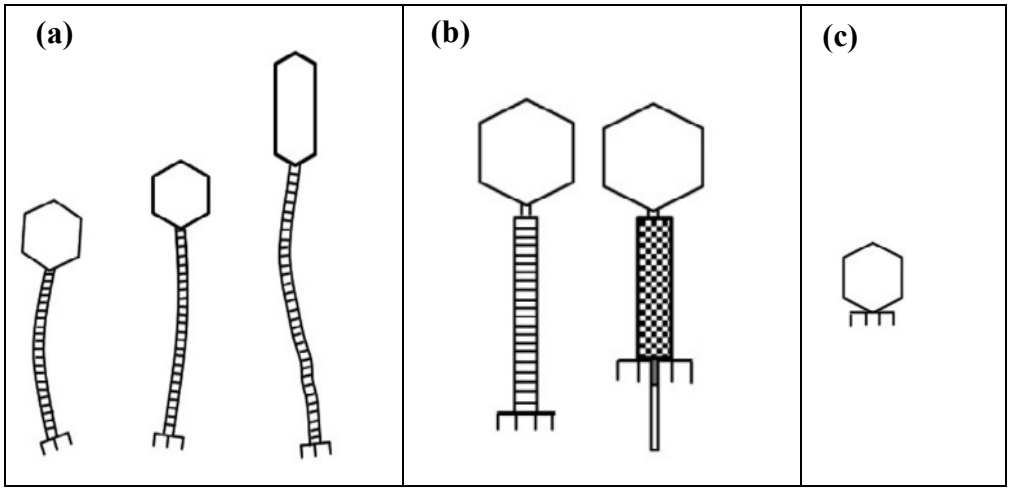

Figure 1-3 The representative phages morphology. Siphoviridae (a), Myoviridae (b), and Podoviridae family (c) (Xia and Wolz 2014)

According to the International Committee on Taxonomy of Viruses (ICTV) (ICTV 2019), a new classification has been updated. The most well-studied *Kayvirus* genus (representative phage K) was updated from *Spounavirinae* subfamily of *Myoviridae* family to *Twortvirinae* subfamily of *Herelleviridae* family. Similarly, *Twortvirus* (representative phage Twort) and *Silviavirus* (representative phage Remus) were also updated into *Herelleviridae* family.

In most *S. aureus* strains, wall teichoic acid (WTA), the most abundant molecule found in the outermost layer of bacterial cell envelopes, is composed of repeated units of ribitol phosphate (RboP) modified by D-alanine and *N*-acetylglucosamine (GlcNAc). The GlcNAc residues are transferred to WTA by the β-GlcNAc transferase TarS and α-GlcNAc transferase TarM (Xia et al. 2010) (Fig. 1-4) (Swoboda et al. 2010; Azam and Tanji 2019b). The WTA attaches to the peptidoglycan by the linker which is synthesized by the initiative of the glycosyltranferase TarO (transferring GlcNac).

Moreover, WTA serves as the main receptor for most of the *S. aureus* phages (Azam and Tanji 2019a). Members of genus *Kayvirus* such as ϕSA012 and phage K require backbone of WTA. While ϕSA039 which is in the same genus requires backbone and β-GlcNAc as its host receptor and recognition site on the *S. aureus* cell wall.

Phage adsorption is mediated by phage receptor binding proteins (RBPs) and receptors on the bacterial cell surface. This primary step is critical for determining the success of phage infection (Silva et al. 2016). Fig 1-5 represents the typical structure of phage and phage DNA insertion into a host cell through the cell wall.

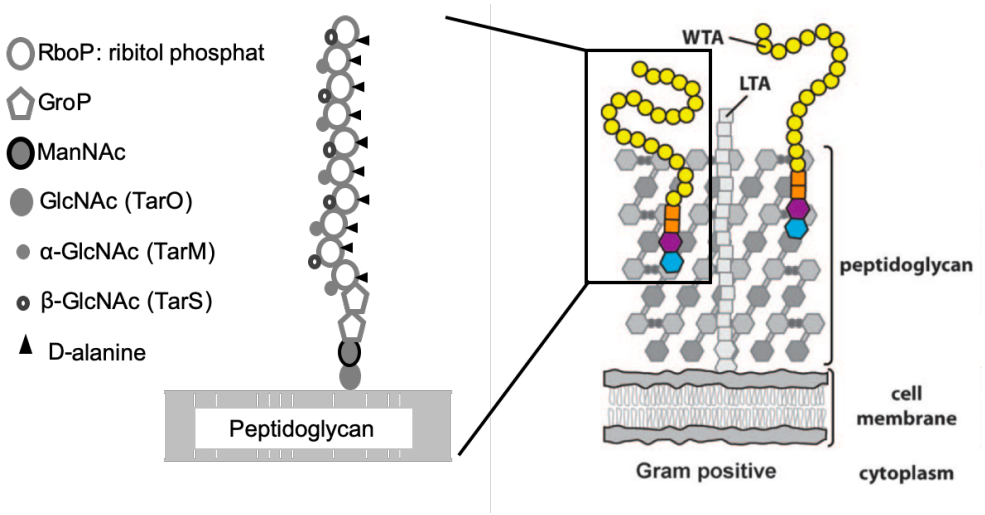

Figure 1-4 WTA structure of *S. aureus* (Swoboda et al. 2010; Azam and Tanji 2019b). Glycerolphosphate (GroP); *N*-acetylmannosamine (ManNAc)

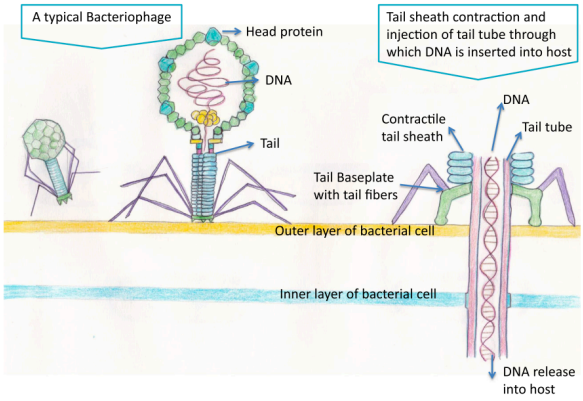

Figure 1-5 Typical structure of a phage emphasizing tail region and contractile ability to insert its DNA into a host (Sharma et al. 2017)

1.6 Enzymes and mechanisms employed by phages to breach the bacterial cell barriers

The initial step of phage infection is the recognition of phage RBPs to the specific host receptor on the host cell surface. This is followed by the phage genome penetration to the site of replication within host cells, the genome assembly to form new virus particles and finally, virion progeny escape from the host cell. Therefore, during an infection cycle, viruses need to overcome the host cell envelope at least twice, first to get inside cells and then to escape from them after virus multiplication (Fernandes and São-José 2018).

Most of the Gram-positive bacteria have lipoteichoic acids anchored to the cytoplasmic membrane via a glycolipid anchor, with a phosphate-rich polymeric moiety extending through the cell wall (Percy and Gründling 2014; Fernandes and São-José 2018). The major structural component of the cell wall is peptidoglycan, also known as murein, which forms a polymeric network surrounding the cytoplasmic membrane (Brown et al. 2013; Fernandes and São-José 2018). In Gram-positive bacteria, the peptidoglycan is also covalently modified with carbohydrate polymers, frequently with anionic WTA (Brown et al. 2013; Fernandes and São-José 2018) (Fig. 1-6).

Some phages synthesize enzymes that attack the bacterial peptidoglycan during the infection process. Those enzymes are known as virion-associated peptidoglycan hydrolases (VAPGHs) or virion-associated lysin (VALs), are phage-encoded lytic enzymes that specifically degrade peptidoglycan. The peptidoglycan-degrading enzymes can be classified into three major groups according to the bond they cleave in the murein network: glycosidases, amidases, and peptidases. Glycosidases cleave one of the two glycosidic bonds in the glycan chain and can be subdivided into *N*-acetyl-β-D-glucosaminidases (glucosaminidases domain), *N*-acetyl-β-D-muramidases

(muramidases or lysozymes) and lytic transglycosylases (Fig. 1-7). The peptidoglycan amidases hydrolyze the amide bond between the first amino acid residue of the peptide stem (generally L-Ala) and NAM, while peptidases cleave within or between the peptide strands. Peptidases are subdivided into carboxypeptidases, which remove C-terminal amino acid residues, and endopeptidases that cleave internal bonds of the peptide (Fig. 1-7).

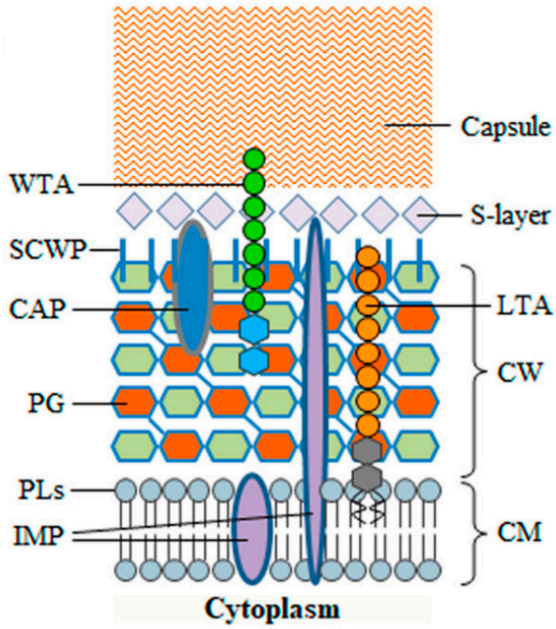

Figure 1-6 Schematic representation of the structure of the bacterial cell envelope in Gram-positive bacteria. SCWP: secondary cell wall polymers; CAP, covalently attached protein; PG: peptidoglycan; PLs: Phospholipids; IMP: inner membrane proteins; CM: cytoplasmic membrane; CW: cell wall; LTA, lipoteichoic acids; The S-layer and capsule are extracellular structures (Fernandes and São-José 2018)

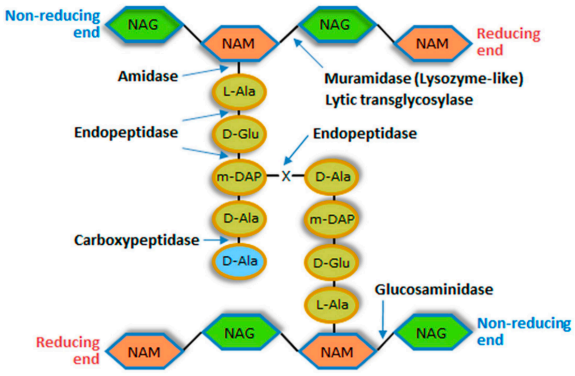

Figure 1-7 Basic structure of the bacterial cell wall peptidoglycan and the cleaving bond of the enzymatic activities of the peptidoglycan degrading enzymes (Pires et al. 2016)

VALs most often correspond to individual components or to domains of tail proteins, like the tape measure protein, central fibers, tail tip knobs, and tail tip puncturing devices, but they can also be capsid inner proteins that are ejected upon virus opening (Pires et al. 2016). An example of virion structure and VAL action is found in *E. coli* phage T4 and its contractile tail. Irreversible binding to host receptors induces tail sheath contraction that cause the inner tail tube with a puncturing device at its tip to penetrate the bacterial cell envelope. One of the proteins composing the piercing apparatus is gp5 that has muralytic activity (Hu et al. 2015).

Moreover, VALs promote a local digestion of the peptidoglycan in order to facilitate penetration or extension of the tail tube to cross the cell wall. Some reported phages which their virus particle are harbored with a VAL (e.g., *E. coli* phage T7, mycobacteriophage TM4 and *S. aureus* phage phi11). The presence of the lytic enzyme in their virion was shown to be important for infection in the laboratory conditions (Moak and Molineux 2000; Piuri and Hatfull 2006; Rodríguez-Rubio et al. 2013; Fernandes and São-José 2018). Importantly, VALs facilitate phages to infect cells which have a thickening and/or increased cross-linking peptidoglycan (e.g., under stationary growth or low temperature) (Moak and Molineux 2000; Piuri and Hatfull 2006; Rodríguez-Rubio et al. 2013; Fernandes and São-José 2018).

1.7 Application of bacteriophage

Due to a crisis of emergence of the antibiotic-resistant pathogen, phage has become attractive as an alternative therapeutic agent to the antibiotic which can be used in various field of application. In biotechnology aspect, phage has been used as a substitute for the antibiotic to control antibiotic-resistant bacteria, as biocontrol agents in agriculture and food safety as well as in aquaculture. Phage also important in medicine and clinical application such as use as a therapeutic agent to treat staphylococcal infection both in vitro and in vivo (Sharma et al. 2017; Azam and Tanji 2019a). In order to obtain a high bactericidal effect, the use of phage cocktails consisting of several phages that bind to different host receptor has been proposed (Synnott et al. 2009). The use of phage cocktail may reduce the inactivation of phage by the immune system and the emergence of phage-resistant bacteria (Azam and Tanji 2019a). Similarly, combined of phage with antibiotic also suggests a synergy effect in controlling bacterial pathogens (Torres-Barcel and Hochberg 2016; Kumaran et al. 2018).

1.8 Aim of this study

Appropriate phage selection is crucial to the success of phage therapy. A wide host range is essential for a phage therapy candidate and a crucial component of phage therapy research. Due

to the limitation of a broad host range phage and the need for phage therapy candidate against clinical MRSA, this study aims to:

1. Isolate phage which has a broad host range against MRSA of human origin
2. Analyze host-recognition mechanism of the newly isolated phage
3. Study the synergistic effects of the isolated phage and antibiotic on controlling of MRSA of human origin.

1.9 Structure of the thesis

Fig. 1-8 shows the structure of the thesis composing of 6 chapters.

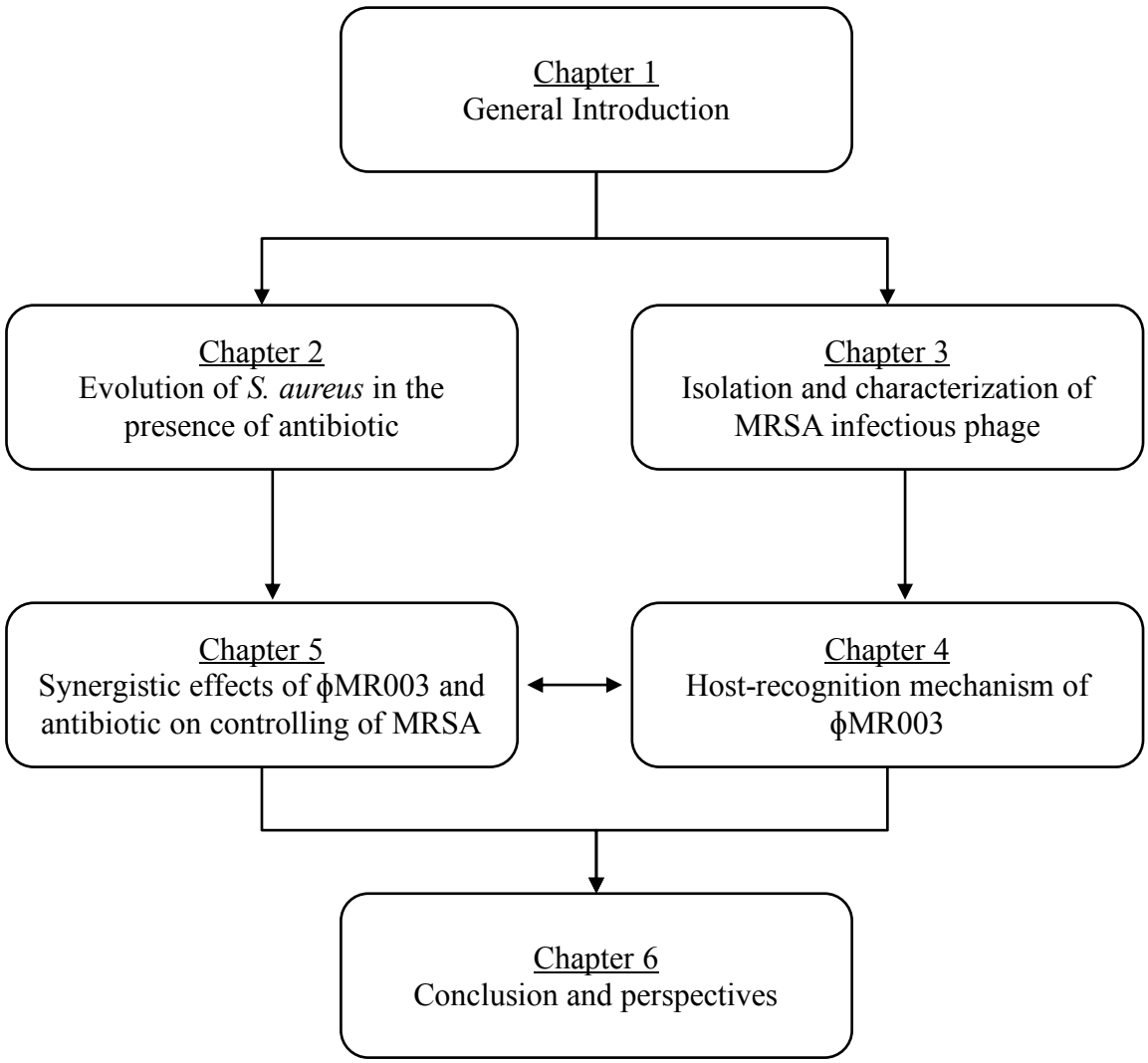

Figure 1-8 The structure of the thesis

2 CHAPTER 2 Evolution of *S. aureus* in the presence of the antibiotic

2.1 Introduction

Antibiotic-resistant bacteria can evolve through the multiple mutation accumulations under stress environment, such as an antibiotic. Antibiotic-resistant evolution through spontaneous mutation can confer higher resistant to the antibiotic from just a single mutation. However, for most of the antibiotics, multiple mutations are required to develop high levels of resistance (Toprak et al. 2011).

S. aureus can develop resistance through horizontal gene transfer by acquiring a resistant gene from the resistant strain. The resistant mechanism includes β-lactamase production, antibiotic target alteration, efflux pumps, and so on. *S. aureus* also develops resistant through spontaneous mutation (Tang et al. 2014). The detection of the resistant mechanisms and their genetic evolution under antibiotic stress is an important support to antibiotic susceptibility surveillance in *S. aureus*. This chapter aims to trace *S. aureus* evolution under stepwise batch culture with the antibiotic.

2.2 Materials and methods

2.2.1 Bacterial strains, antibiotic and mediums

A drug-sensitive wild type (WT) strain *S. aureus* ATCC6835 was adapted to increased concentration of oxacillin (Wako, Japan). Cation Adjusted Mueller Hinton broth (CAMHB) supplemented with 2% of NaCl was used in the stepwise batch culturing of the *S. aureus* ATCC6835 with oxacillin and Minimum Inhibitory Concentration (MIC) test.

2.2.2 Batch culturing of *S. aureus* ATCC 6538 with increased dose of oxacillin

An overnight culture of *S. aureus* ATCC 6538 was inoculated 1% into L shaped tube in a series of increased concentration of oxacillin (Figure 2-1). The cultivation was conducted in TVS062CA compact rocking incubator (ADVANTEC, Tokyo, Japan) at 35℃ with shaking 40 rpm in CAMHB supplemented with 2% of NaCl. Optical density (OD_{660}) value of cultivation was automatically recorded in every 15 min at 660 nm wavelength. One culture without oxacillin was used as a control. The cultivation period was conducted until the culture reached stationary phase (needs several days). The culture where bacterial growth was present at the highest concentration was used as serial transfer inoculum into fresh medium for the next concentration challenge. Each

serial transfer with increased concentration challenges was called round. Totally, 17 rounds were conducted.

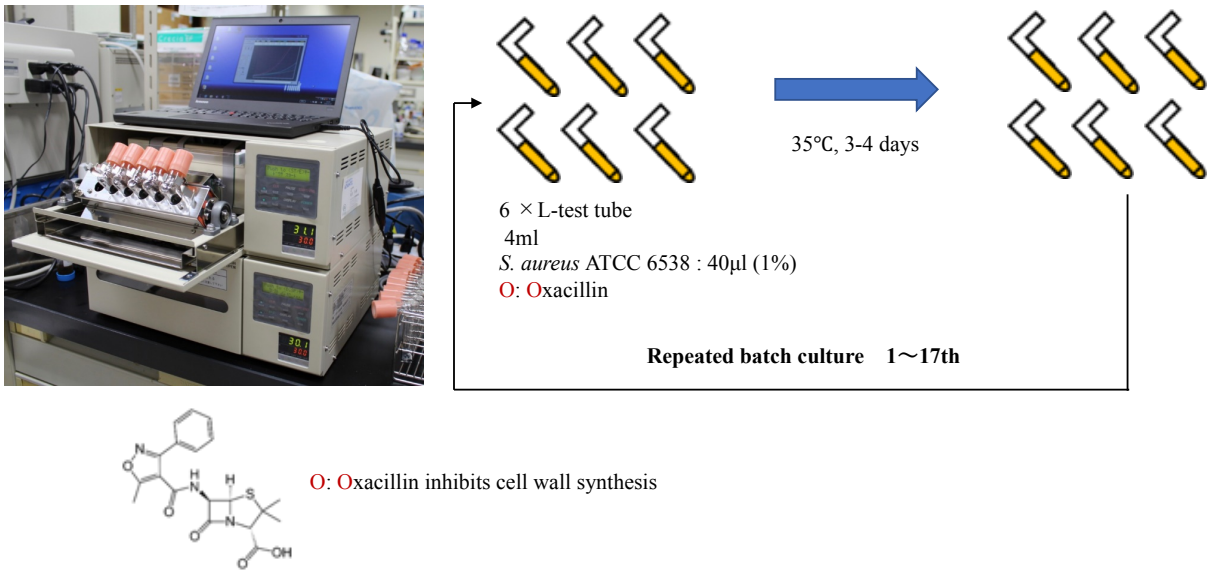

Figure 2-1 Batch culture of *S. aureus* ATCC 6538 with the increased dose of oxacillin

2.2.3 MIC and Cross-resistant test

The MIC and Cross-resistant test were conducted according to Clinical Laboratory Standard Institute (CLSI) protocol with some modification (CLSI 2012). An overnight culture was adjusted to concentration of 10^6 Colonies Forming Unit (CFU) per ml using CAMHB medium supplemented with 2% of NaCl for testing with oxacillin or without supplement of NaCl for testing with vancomycin (Wako, Japan), kanamycin (Wako, Japan), ciprofloxacin (Wako, Japan), and erythromycin (Wako, Japan). All of the antibiotics used belong to different classification. The vancomycin belongs to glycopeptide which targets the precursor of cell wall. The ciprofloxacin belongs to the fluoroquinolones which targets the DNA gyrase. The kanamycin belongs to aminoglycoside which targets the 30S rRNA and the erythromycin that belongs to macrolides targets the 50S rRNA (Bal and Gould 2005). The adjusted overnight cultures were transferred into 96 microwell plates with the pre-two-fold dilution of antibiotic concentration. The final concentration of the culture was in between 2-8 x10^4 CFU/ml in each well. The cultures were incubated for 24h at 35°C. The MIC was determined by the minimum concentration of antibiotic which prevents the visible growth of the bacteria after the incubation.

2.2.4 Whole-genome analysis and bioinformatics

WT strain and its mutant strains which were recovered from the repeated batch culture, were

extracted their genome by using GenElute Bacterial Genomic DNA kits (Sigma, Germany). Next, the genome was submitted for analysis by illumination Miseq at Hokkaido System Science (Japan). The sequence reads of WT were mapped to the reference strain *S. aureus* ATCC 6538 available in the database with the accession number CP020020 by Burrows-Wheeler Aligner (BWA) (Li 2013). Next, the mapped genome sequence of WT was used as a reference for mapping with the mutant strains by BWA and Single Nucleotide Polymorphisms were detected by SAMtools/BCFtools (Li et al. 2009) and Pilon (Walker et al. 2014). Open Reading Frames (ORFs) were predicted and annotated by using the RAST server (http://rast.nmpdr.org/).

2.3 Results

2.3.1 Batch culture of *S. aureus* ATCC 6538 with the oxacillin

(a)

Serial transfers	Oxacillin concentration (µg/ml)																	
	0.031	0.062	0.125	0.25	0.5	1	2	4	8	16	32	50	100	200	400	800	1600	3200
1	O	O	O	O	O													
2					Δ	O	Δ	Δ	Δ									
3							O	O										
4								O*	O	O	Δ	Δ						
5										O	O	x	Δ	Δ				
6											O	O	Δ	Δ	x			
7												O	O	Δ	x	x		
8													O	O	Δ	x	x	
9														Δ	O	x	x	x
10															Δ	O*	x	x
11																O	x	x
12																O	Δ	x
13																O	Δ	x
14																O	x	x
15																O	x	x

(b)

Round	Oxacillin concentration (µg/ml)																			
	0.031	0.062	0.125	0.25	0.5	1	2	4	8	16	32	50	100	200	400	800	1000	1200	1400	1600
16																O	O	O		
17																		O	O	Δ*

Figure 2-2 Summary of the stepwise batch culture of *S. aureus* ATCC 6538 with oxacillin. The concentration of oxacillin was increased from one batch to another with a total of 17 batch cultures. (a) round 1-15; (b) round 16-17; O: $OD660_{660}$ >1 at stationary phase after incubation; Δ: OD_{660}<1 at stationary phase after incubation, x: no growth observed. Shade indicates the seed used for the next batch culturing; * indicates the culture where the mutant strains were screen.

Fig. 2-2 shows the total batch culture of *S. aureus* ATCC 6538 with stepwise increasing oxacillin concentration. In round 1, all of the oxacillin concentration allowed the growth of the bacteria even in the concentration higher than oxacillin-MIC (Fig. 2-3, round 1). The MIC of WT is 0.062 µg/ml of oxacillin. With the increased oxacillin concentration up to 8 µg/ml, the cell was not able to grow well in round 2 (Fig. 2-3).

With the concentration of 2 µg/ml or lower, the cell could grow but the growth rate was lower than the culture without oxacillin in round 2 (Fig. 2-3). In the 3rd batch, the cell that grew at 2 µg/ml, was used as inoculum with 2 times increased concentration of oxacillin. The cell was able to grow at the concentration that was previously grew and the 2 times increased concentration of oxacillin (4 µg/ml) (Fig. 2-2).

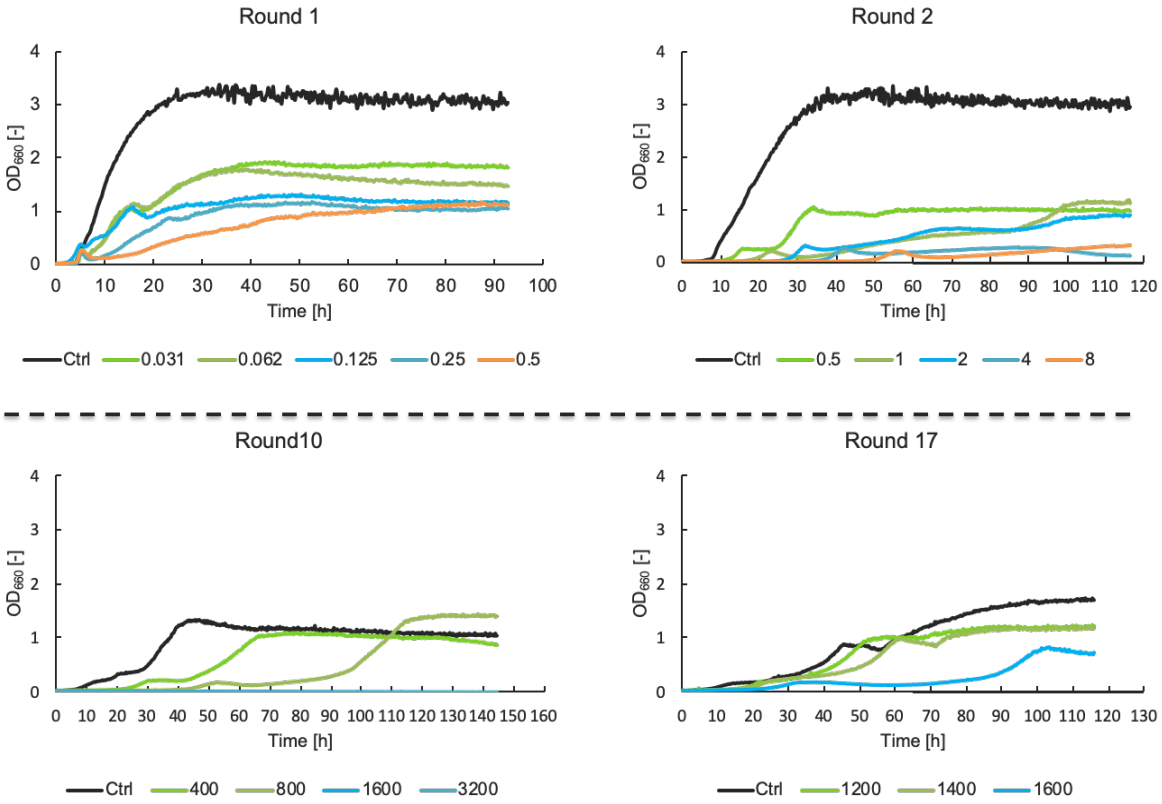

Figure 2-3 Growth curve in batch culture of *S. aureus* ATCC 6530 with the oxacillin. 4 batch cultures were selected as representative. Ctrl: culture without oxacillin. Value of the legend represents the concentration of oxacillin used.

Next, the culture at the highest concentration (4 µg/ml) in which the cell grew, was used as the seed for the following round. With this criterion, the highest concentration which the cell could grow was at 1600 µg/ml at the 17th round. From round 4 until round 9, the bacteria could grow at 2 times increase of the oxacillin concentration from which they grew. However, until reaching

800 µg/ml (round 10), the cell was not able to grow at concentration higher than 800 µg/ml (Fig. 2-2).

Next, several batch cultures were repeated with the same oxacillin concentration to the round 10 in the presence of oxacillin dose up to 3200 µg/ml. But the bacteria could not grow at this concentration. The oxacillin concentration reduced to 1200 and 1600 µg/ml in the round 16 and 17, respectively. The decreased concentration of oxacillin allowed bacteria to grow.

By repeating 17 times batch cultures, the bacteria cell was able to grow at the highest concentration of 1600 µg/ml. However, the growth rate was slower than the culture with lower concentration (Fig. 2-3) (Round 17).

2.3.2 MIC and cross-resistant of mutant strains

The oxacillin-MIC of *S. aureus* ATCC6538 was 0.062 µg/ml which indicates that the strain is a drug-sensitive. According to CLSI (CLSI 2012), MIC breakpoint of *S. aureus* is determined as resistant when they grow with the a concentration of oxacillin equal to or higher than 4 µg/ml or susceptible with concentration lower or equal to 2 µg/ml. The MIC breakpoint based on CLSI of the antibiotics used are listed in Table 2-1.

The round 4, 10 and 17 which the culture was exposed to 4, 800 and 1600 µg/ml of oxacillin, respectively, were selected to isolate the mutant strains by picking the single colony. The cross-resistant of mutant isolates was conducted. Table 2-1 shows the cross-resistant of the selected mutant isolates to oxacillin and other classes of antibiotics. CLSI-MIC of each tested antibiotic is different. The mutant strains were resistant to oxacillin but not cross-resistant to other antibiotics tested. MIC of C4 and C800 increased up to 100 and 1600 µg/ml of oxacillin, respectively. MIC of C1600 toward oxacillin was not able to determine because of the slow growth of the mutant strain during the long storage period. At the high concentration of MIC test, the mutant strain isolated from 1600 µg/ml was slow growth so that it was difficult for MIC judgment. But considering that this strain was recovered from the culture of 1600 µg/ml of oxacillin, its MIC was considered higher than this concentration.

Table 2-1 MIC of WT ATCC6538 and its mutants to different antibiotics

Antibiotic	CLSI-MIC	MIC			
		WT	C4	C800	C1600
Oxacillin	4	0.062	100	1600	n/a
Vancomycin	16	0.25	0.25	0.25	0.25
Ciprofloxacin	4	2	1	1	1
Kanamycin	64	4	4	1	4
Erythromycin	8	0.125	0.125	0.062	0.062

n/a not available

2.3.3 Whole-genome analysis of mutant strains

Based on whole-genome analysis of mutant strains compared to WT, spontaneous mutations were found conferring resistant to oxacillin (Table 2-2). The mutations which conferred silent mutation was not discussed. The mutations which were outside of ORF were excluded except mutations that were related to a promoter.

Table 2-2 presents the mutations in mutant strains C4, C800 and C1600 compared to WT strain. The fictional protein encoding in mutated genes were search in BLAST search. The strain C4 harbored less mutations than the strain C800 and C1600. Some mutations existed in all of the three strains such as gene *rpo*D encoding RNA polymerase sigma factor; gene *yvg*F encoding cell wall-active antibiotic response protein; gene *tet*R/*acr*R encoding DNA-binding transcriptional regulator. Mutation in gene *pbp*4 encoding penicillin binding protein was found only in strain C4. Several mutations by insertion in gene *tar*O encoding glycosyltransferase responsible for initiation of WTA synthesis, were observed in strain C800 and C1600. Mutation in *rnh*C encoding Ribonuclease HIII that is responsible for DNA replication and repair, was observed in both strain C800 and C1600. While mutation in gene *val*S encoding valine tRNA ligase was found only in strain C1600.

Table 2-3 shows mutation by the deletion in the strain C4, strain C800 and strain C1600. The strain C4 contained less deletion compared to strain C800 and strain C1600. However, strain C800 had more deletion mutation than strain C4 and strain C1600. While in strain C4, the partial deletion was observed just in *lyt*R gene. There was no deletion in *fmt*A gene was observed in C4. Moreover, strain C800 and C1600 acquired a whole deletion of *lyt*R gene and a partial of *fmt*A gene. C800 harbored additional deletion in *mutS2* gene.

Table 2-2 Spontaneous mutation in mutant stains

Position WT	Amino acid		Mutant strains			Gene	Accession number
	WT	ALT	C4	C800	C1600		
663449	TTC (F)	TCC (S)	○	x	x	*pbp*4	AYU98954.1
1584053	TGT (C)	TAT (Y)	○	○	○	*rpo*D	WP_064264749.1
1931576	GCA (A)	GAA (E)	○	○	○	*yvq*F	VFS07056.1
2569725	G	GG	○	○	○	*tet*R/*acr*R	WP_070021141.1
772974	.	AACTAC (N) (Y)	x	○	○	*tar*O	WP-112380577
1098187	.	T	x	○	○	*rnh*C	WP_079199726.1
1674767	TGG (Y)	TCG (S)	x	x	○	*val*S	WP_042727698.1

○: present, x: absent, ALT: alternation, underline: insertion

Table 2-3 Deletion in mutant strains

Position in WT (deletion length in bp)	Deletion			Gene	Accession number
	C4	C800	C1600		
1009831-1012173 (2343 bp)	∆	○	○	*lyt*R; *fmt*A	WP_031871891.1
1103641-1104552 (912 bp)	x	○	x	*mut*S2	VDZ34952.1

○: present, x: absent, ∆: partial deletion in *lyt*R gene

2.4 Discussions

This chapter describes the possible resistant mechanism of mutant *S. aureus* recovered from the stepwise batch culture of *S. aureus* ATCC 6538 with oxacillin. This study revealed that antibiotic-sensitive *S. aureus* developed into antibiotic-resistant strain through spontaneous mutation during the stepwise batch culturing which is similar to previously reported (Toprak et al. 2011; Schenk and de Visser 2013; Lenhard et al. 2015). The MIC of the mutant strains were higher than the standard MIC breakpoint of being resistant (Table 2-1). Moreover, the mutant strains did not confer resistant to other classes of antibiotic (Table 2-1). The horizontal gene transfer plays a crucial role in distributing antibiotic resistant gene among *S. aureus*. However,

the reported resistant mechanism to all known classes of antibiotics has been linked to genes found within the *S. aureus* chromosome or due to spontaneous mutation resulted from selection pressure (Espedido and Gosbell 2012).

Based on whole genome analysis in mutant strains, various mutations, insertion and deletion were observed (Table 2-2, Table 2-3). In strain C4, mutation in PBP4 which is one of an important enzyme involves in peptidoglycan synthesis was observed (Vollmer et al. 2005). Since oxacillin targets PBPs, in order to escape from the oxacillin, *S. aureus* often mutates in this gene (Foster 2017). The mutation in gene *pbp*4 was not found in strain C800 and strain C1600, which implies that mutation is random among strains. Nevertheless, the three mutant strains acquired the same mutation in gene *yvq*F encoding cell wall active antibiotic response protein in *S. aureus*, especially in MRSA. This protein induced MRSA resistant expression to the methicillin, vancomycin, and daptomycin (Boyle-Vavra et al. 2013). Moreover, a protein encoded in YvqF facilitates resistance by playing a necessary regulatory role in the VraSR (regulatory system) that is a cell wall stimulant mediator. The VraS and VraR autoactivate the expression of the vra operon and about 46 other unlinked genes in the vra regulon, several of which encode known or putative cell wall biosynthesis enzymes that can presumably repair cell wall damage (Boyle-Vavra et al. 2013). Thus, the protein encoded in *yvq*F help to repair the damaged cell wall caused by the antibiotic (Boyle-Vavra et al. 2013). Deletion in gene *fmtA* gene was observed in strain C800 and strain C1600. This protein encoded in *fmt*A plays an important role in cell wall synthesis and methicillin-resistant in MRSA (Rahman et al. 2016). Deletion of gene *fmt*A gives abnormality of cell growth (Rahman et al. 2016). Although the deletion of this gene did not affect antibiotic resistance in the mutant strains (strain C800 and C1600), the slow growth of strain C800 and C1600 were observed.

CHAPTER 3 Isolation and characterization of MRSA infectious phage

3.1 Introduction

The emergence of life-threatening MRSA has led to increased interest in the use of bacteriophages as an alternative therapy to antibiotics (WHO 2014). Phage therapy gives several advantages over the antibiotic treatment such as phage infectivity is host specific so that phage cannot kill the other microflora. The possibility of phage to kill its host is high and it is suitable to use on antibiotic allergies patient. Moreover, if phage-resistant strains emerge, the phage mutates to counter adapt with the host (Gordillo Altamirano and Barr 2019).

Phages with wide host ranges that target clinical MRSA strains are limited (Gu et al. 2019). Appropriate phage selection is crucial to the success of phage therapy. A wide host range is essential for a phage therapy candidate and a crucial component of phage therapy research.

In this chapter, I describe the isolation of phage ϕMR003, which has a broad host range against clinical MRSA. The genome and general features of ϕMR003 were characterized.

3.2 Materials and methods

3.2.1 Bacterial strains, bacteriophage isolation, and culture conditions

S. aureus strain RN4220 was provided by Prof. Motoyuki Sugai (Hiroshima University, Graduate School of Biomedical & Health Science, Hiroshima, Japan), with the permission of Prof. Richard P. Novick (Skirball Institute of Biomolecular Medicine, NY) and used as a host for phage enrichment. RN4220 is a competent strain used in the laboratory whose parent strain is the clinical isolate, *S. aureus* strain NCTC8325. *S. aureus* strain SA003, previously isolated from bovine mastitic milk (Synnott et al. 2009), was also used. Details of the strains used are listed in Table 3-1.

To determine host range, 104 strains of MRSA clinical isolates were randomly selected from MRSA strains, of which the MIC was more than 4 μg/ml of oxacillin following to the criteria of the Clinical and Laboratory Standards Institute (CLSI 2012), of Kyorin University Hospital (Tokyo, Japan) in 2015 and 2016. The MRSA strains were classified into HA-MRSA or CA-MRSA according to the SCC*mec* type based on the phage open reading frame (ORF) typing by POT kit (Kanto Chemical Co., Inc., Tokyo) (Suzuki et al. 2009b; Maeda et al. 2012). This kit detects phage-derived ORFs which allows us to understand the genotypes of strains widespread

in specific regions during an outbreak. POT has three scores that indicate different features of MRSA, such as SCC*mec*, prophage, and genomic island (Suzuki et al. 2009b; Suzuki et al. 2009a). Among these, the POT1 score is used to differentiate SCC*mec* types.

Table 3-1 Bacterial strains and phages

Strain name	Description	Reference
S. aureus RN4220	Transformable strain, restriction-deficient (*hsdR*$^-$), *rsbU*$^-$, *agr*$^-$	DSM 26309, DSMZ culture collection, Braunschweig, Germany
S. aureus SA003	*S. aureus* isolated from bovine mastitic milk	(Synnott et al. 2009)
ϕSA012 and ϕSA039	Isolated from sewage influent in Tokyo possess a broad host range phage against bovine mastitis *S. aureus*	

Phage was isolated from the influent of a municipal wastewater treatment plant in Tokyo, Japan. The isolation method was previously described (Synnott et al. 2009). Strain RN4220 was used as the primary phage propagation host for newly isolated phage. SA003 was used as the propagation host for previously isolated phages ϕSA012 and ϕSA039 (Synnott et al. 2009) (Table 3-1). Phage purification was conducted by repeated plating and picking of single plaques, followed by plate lysate and the polyethylene glycol (PEG) #6000-NaCl precipitation method (Synnott et al. 2009). Phages ϕSA012 and ϕSA039 were used for comparison to the newly isolated MRSA infectious phage ϕMR003. All bacterial strains and phages were grown in Luria-Bertani (LB) (10 g of NaCl, 10 g of Hipolypepton and 5 g of Yeast extract per litter) medium overnight at 37°C, unless otherwise stated.

3.2.2 Phage host range (spot test)

One hundred and four MRSA isolates were used to test the infectivity of ϕMR003, whose host range was subsequently compared to those of ϕSA012 and ϕSA039. RN4220 was a primary host and used as the control strain for ϕMR003. SA003 was a primary host and used as the control strain for ϕSA012 and ϕSA039. To determine the infectivity of the phages on the bacterial strains, 5 μl of phage lysate at titer 10^6, 10^5, and 10^4 plaque forming units (PFU) was dropped onto an agar plate with *S. aureus* mixed with 0.5% (w/v) top agar and incubated overnight. Infectivity was determined by the turbidity of plaques where the phage lysate was dropped.

3.2.3 Phage morphology

Phage morphology was observed by transmission electron microscopy (TEM). Phage-containing lysate was purified by PEG #6000- NaCl precipitation and CsCl centrifugation using previously described methods with modifications (Synnott et al. 2009). Briefly, 5 µl of a concentrated phage suspension with a minimum of 10^9 PFU/ml in SM buffer (100 mM NaCl, 8 mM $MgSO_4$, 50 mM Tris-HCl, and 0.01% (w/v) gelatin, pH 7.5) was spotted on a hydrophilic plastic-carbon-coated copper grid (Nissin EM Corporation, Tokyo, Japan). Phages were allowed for 1 min adsorption. Excess sample was removed by carefully touching the side of the grid with filter paper. Next, 10 µl of distilled water was spotted on the grid and removed after a short time. Phages were stained by adding 5 µl of 2% (v/v) uranyl acetate or EM Stainer (Nissin EM Corporation, Tokyo, Japan). After 1 min, the excess stain was removed, and the grid was air-dried for 30 min. The grids were observed with a transmission electron microscope (JEM-1400 Plus, JEOL Ltd, Tokyo, Japan) operating at 80 kV.

3.2.4 Single-step growth

Single-step growth was conducted using a previously described method with some modifications (Osada et al. 2017). Phage was added to the bacterial culture to achieve a multiplicity of infection (MOI) of 0.01 in a total volume of 2 ml, and 10 minutes were allowed for phage adsorption. After adsorption, the culture was washed with LB broth five times on ice to remove free phages. Washed cells with adsorbed phage were incubated again in 2 ml of LB at 37 ºC with shaking at 120 rpm. One hundred microliters of culture were removed periodically at 0, 5, 10, 15, 20, 25, 30, 35 and 40 min and used to perform plaque assays against RN4220. The first sampling time after the wash step was defined as time zero. By observing time courses of the number of adsorbed phages plus released phages from lysed host cells, a single-step growth curve was generated. The ten min allowed for phage adsorption was added to the latent period calculation from the single-step growth curve generated and burst size was determined. The phage titer was normalized by the initial phage titer.

3.2.5 DNA extraction, sequencing, and bioinformatics

DNA was extracted from phages as previously reported (Takeuchi et al. 2016). Briefly, the phage genome was extracted from purified phage using a phage DNA isolation kit (Norgen Biotex Corp., Thorold, ON, Canada). Genomes were submitted to BGI (Hongkong) for whole genome sequencing by Illumina HiSeq platform with genome coverage (sequencing depth) of 100-fold

with 100 bp paired-end. Sequencing results were assembled and aligned using Velvet ver. 1.2.10 (Zerbino and Birney 2008). Pairwise sequence alignments (nucleotide) were performed with EMBOSS Stretcher (Myers and Miller 1988; Rice et al. 2000).

3.2.6 Accession number(s)

The genomic sequence of ϕMR003 was submitted to the DNA Data Bank of Japan (DDBJ) database under the accession number AP019522. The genomes of ϕSA012, ϕSA039, and SA003 were available in the GenBank database under accession numbers AB903967, AP018375, and AP018376, respectively.

3.3 Results

3.3.1 Characteristics of selected MRSA isolates

Based on the POT test, all selected clinical MRSA strains from Kyorin University Hospital were classified into SCC*mec* types I, II, and IV based on POT1 score. SCC*mec* types I and II are categorized as HA-MRSA while type IV is categorized as CA-MRSA. POT testing revealed that SCC*mec* type II strains are the New York/Japan strain and six SCC*mec* type IV strains are USA300. Furthermore, other unknown strains harbored SCC*mec* I or IV, showing distinct POT scores revealing different phenotypes.

3.3.2 Isolation of lytic phages and host range

Municipal wastewater was used to screen phages, which resulted in the isolation of various lytic phages against RN4220. As we were attempting to isolate phages with a wide host range, we tested several of the phages we recovered against representative MRSA strains using spot test assay. As a result, we found that one of the phages we had isolated, ϕMR003, showed high infectivity against all representative MRSA strains, indicating that we had found a promising phage candidate for MRSA treatment. For comparison, previously isolated phages, ϕSA012 and ϕSA039 (showed high infectivity against *S. aureus* isolated from bovine mastitic milk) (Synnott et al. 2009), were also tested against MRSA. We used ϕSA012 and ϕSA039 to infect MRSA collection because both phages belong to *Kayvirus*, a genus which presents in most commercial phage preparation which has been widely used (Azam and Tanji 2019a).

Phage host range was determined by the spot test assay. Phage solution with different titers of 10^6, 10^5, 10^4 PFU were spotted on a bacterial lawn. The infection was determined by the

formation of clear plaques. Based on spot test results, RN4220 showed high sensitivity to ϕMR003 (clear plaque) but lower sensitivities toward ϕSA012 and ϕSA039 (turbid plaque). In contrast, SA003 showed high sensitivity to ϕSA012 and ϕSA039 (clear plaque) but is less sensitive to ϕMR003 (turbid plaque).

Table 3-2 Sensitivity of HA-MRSA and CA-MRSA isolates to ϕMR003, ϕSA012, and ϕSA039 by spot test

Prevalence setting	SCC*mec*	ϕMR003	ϕSA012	ϕSA039	Number of strains
HA-MRSA	II	+	+	+	34
	I	+	+	-	1
	II	+	+	-	7
	n/a	+	-	+	0
	n/a	-	+	+	0
	I	+	-	-	1
	II	+	-	-	6
	n/a	-	+	-	0
	n/a	-	-	+	0
	n/a	-	-	-	0
Sub-total		49	42	34	49
CA-MRSA	IV	+	+	+	23
	IV	+	+	-	9
	n/a	+	-	+	0
	IV	-	+	+	2
	IV	+	-	-	20
	n/a	-	+	-	0
	n/a	-	-	+	0
	IV	-	-	-	1
Sub-total		52	34	25	55
Total		101	76	59	104
RN4220	n/a	+	+/-	+/-	1
SA003	n/a	+/-	+	+	1

(+) sensitive (clear plaque); (+/-): medium (turbid plaque); (-): insensitive (no plaque); (n/a): not available

Table 3-2 shows MRSA strains sensitive to ϕMR003, ϕSA012, and ϕSA039 by spot test. ϕMR003 showed a broader host range than ϕSA012 and ϕSA039. ϕMR003 infected all HA-MRSA (49 isolates, SCC*mec* type I and II) and 52 out of 55 of CA-MRSA isolates. Moreover, ϕMR003 highly infected all USA300 strains, which are life-threatening CA-MRSA strains that emerged in the US. In contrast, ϕSA012 and ϕSA039 infected 42 and 34 of HA-MRSA, and 34 and 25 of CA-MRSA, respectively. One other strain of MRSA (MR58) was not sensitive to any of the three phages. Overall, ϕMR003 showed 97% (101/104) infectivity, while ϕSA012 and ϕSA039 showed 73% (76/104) and 57% (59/104) infectivity to MRSA isolates, respectively.

3.3.3 Phage morphology

Based on morphological features as observed by TEM, ϕMR003 is assigned to the *Herelleviridae* family due to the presence of long contractile tail (Fig. 3-1). This phage has an average head diameter of 93 nm, and tail with a length of 210 nm and a width of 22 nm (Fig. 1b), which is close to Remus (Vandersteegen et al. 2013). Specifically, these features correspond to those of other reported *Herelleviridae S. aureus* phages (Klumpp et al. 2010).

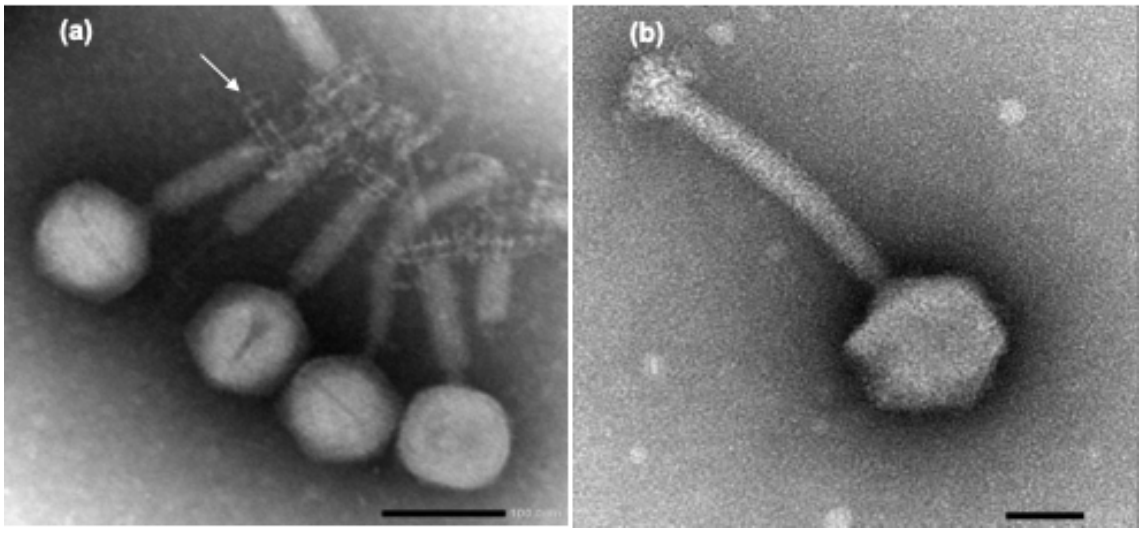

Figure 3-1 Morphology of ϕMR003. (a) Multiple views of ϕMR003, the bar indicates 100 nm, the arrow indicates contract tail; (b) single view of ϕMR003, the bar indicates 50 nm

3.3.4 Single-step growth

Single-step growth was conducted to quantify the phage propagation between ϕMR003 and RN4220. The latent period of ϕMR003 was 33 min. The burst size of ϕMR003 was 35 PFU per cell (Fig. 3-2). This result was comparable to ϕSA012 against SA003, which yielded an average burst size of 41 PFU per cell (Osada et al. 2017). A *Siphoviridae* family SA97 showed similar

features with a latent period of 20 min and a burst size of 32 PFU per infected RN4220 cell (Chang et al. 2015).

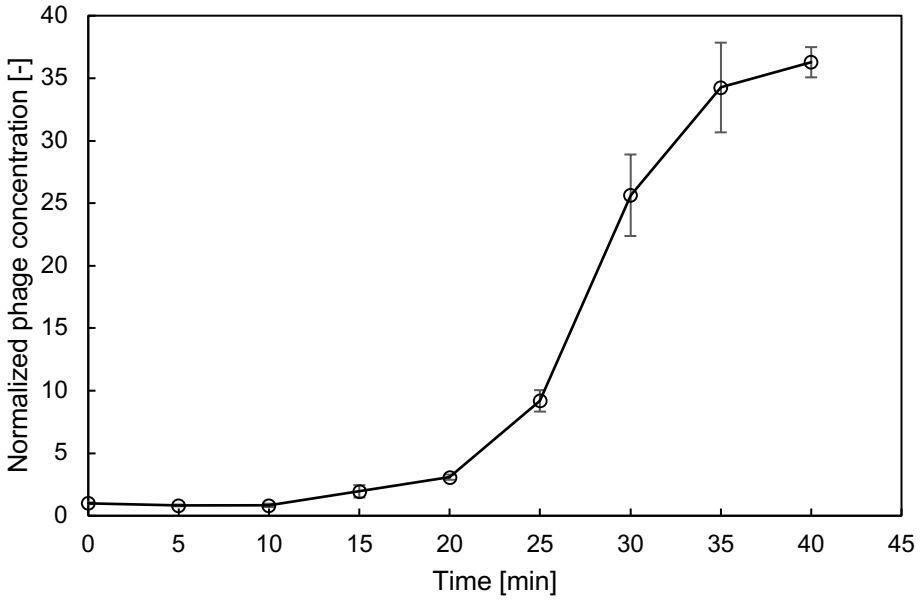

Figure 3-2 Single-step growth of ϕMR003 with RN4220. Time zero represents the time of first sampling after five washes followed by 10-min adsorption, (n = 3, means ± SD)

3.3.5 Genome analysis of ϕMR003

Based on whole genome analysis, ϕMR003 contains a double-stranded DNA comprising 132,152 bp with 185 putative predicted ORFs and 30% GC content. No tRNA gene was detected in its genome. Antibiotic-resistant genes and virulence genes were not detected, suggesting that this phage is safe for phage therapy.

A comparison of the genome of ϕMR003 with those of studied *S. aureus* phages, including Remus (JX846612), SA11 (JX194239), ϕSA012 (AB903967), ϕSA039 (AP018375), and phage K (KF766114) is presented in Fig. 3-3. The genome organization of ϕMR003 is similar to that of Remus (Vandersteegen et al. 2013). ϕMR003 showed 80.2% and 87.1% nucleotide identity to phages Remus and SA11, respectively, in the genus *Silviavirus* (Vandersteegen et al. 2013; Cui et al. 2017). Therefore, ϕMR003 represents a new species within this genus based on the criteria of less than 95% genome similarity to the phage genome available in the database (Adriaenssens and Rodney Brister 2017). In addition, we compared some genome features of Remus to those of ϕMR003, especially genes interrupted by self-splicing elements that were reported as distinct from other phages. In the genome of ϕMR003, the terminase large-subunit gene was fragmented by *orf73* and orf74 which encoded hypothetical proteins. In Remus, the terminase gene is

fragmented into *orf2* and *orf5* which encode group I introns. Therefore, the introns inserted into the terminase gene of Remus are absent in ϕMR003. Similar to Remus, *orf82* and *orf85*, which encode portal proteins of ϕMR003, were fragmented by *orf83* and *orf84*, which encoded transposase. However, the degree of amino acid identity between the transposase of Remus and that of ϕMR003 was under 59% (Vandersteegen et al. 2013). In addition, the helicase gene of ϕMR003 was split into two ORFs (ORF120 and ORF121), a quality similar to Remus (ORF49 and ORF50) (Vandersteegen et al. 2013). In Remus, ribonucleotide reductase large-subunit genes (ORF66, ORF68, ORF70) are interrupted by two group I introns (Vandersteegen et al. 2013). On the other hand, in ϕMR003, these genes were interrupted by one group I intron. ORF148 and ORF150, which encoded the DNA repair protein in ϕMR003, was fragmented by an intron as observed in Remus (ORF80 and ORF82).

	ΦMR003	Remus	SA11	ΦSA012	ΦSA039	K
ΦMR003	100					
Remus	80.2	100				
SA11	87.1	84.6	100			
ΦSA012	54.3	50	52.4	100		
ΦSA039	54.3	48.6	50.7	86	100	
K	53.9	57.9	52.8	83.3	83.1	100

Figure 3-3 Genome comparison between *Silviavirus* (ϕMR003, Remus, and SA11) and *Kayvirus* (ϕSA012, ϕSA039, and phage K)

The genome of ϕMR003 showed about 54% nucleotide identity to those of phages belonging to the genus *Kayvirus*, namely ϕSA012, ϕSA039, and phage K. The Remus genome is very similar to that of SA11, as well as that of ϕMR003 (Fig. 3-3). The genome of Remus and SA11 show less than 60% nucleotide identity to ϕSA012, ϕSA039, and phage K. Moreover, ϕSA012, ϕSA039, and phage K are closely related to nucleotide identities exceeding 80%.

3.4 Discussions

This study described the isolation of ϕMR003 with a broad host range against HA-MRSA and CA-MRSA. Member of *Kayvirus*, including ϕSA012, ϕSA039, K, ISP, and ϕ812, were reported as potential phage candidates for the control of staphylococcal infections (Cui et al. 2017). This study revealed that ϕMR003 belonged to *Silviavirus*, and showed a broader host range against MRSA than ϕSA012, and ϕSA039. ϕMR003 infected 97% of MRSA strains that originated from humans (i.e. 101 out of 104 MRSA strains of human origin). In contrast, ϕSA012 and ϕSA039 infected 73% and 57% of human origin MRSA, respectively. Phage K, ISP, and ϕ812 were reported to infect 61%, 86%, and 83% of *S. aureus* isolates (including MRSA), respectively. Remus (*Silviavirus*) also infected human and animal origin of 70% of the tested *S. aureus* strains (Vandersteegen et al. 2013). The same representative panel of MRSA strains would be essential to assess their different lytic efficiencies. Nevertheless, ϕMR003 has a wide host range against MRSA of human origin in Japan, therefore making it a potential phage candidate for controlling MRSA infections.

4 CHAPTER 4 Host-recognition mechanism of phage ϕMR003

4.1 Introduction

Phages depend on their host for new viral particles production and release inside and outside, respectively. Phage tails are considered as molecular machines that specifically recognize bacterial host cells, penetrate the cell envelope and deliver the phage genome into the cytoplasm (Nobrega et al. 2018). The adsorption of phage onto host cell is the primary step and crucial for phage replication. This process mediated by phage receptor binding proteins (RBPs) and receptors on the bacterial cell surface. The phage recognizes a sensitive host and next positions itself for DNA ejection into the host (Silva et al. 2016). Therefore, this step is critical for not only determining the success of phage infection but also represents the initial point of phage-host contact and the phage's host range specificity (Silva et al. 2016). Despite this usefulness event, the phage-host interaction is poorly characterized.

The outmost layer of gram-positive cell envelopes, such as *S. aureus* consist of WTA that plays as phage receptor for most of the *S. aureus* phages (Xia and Wolz 2014). There are two major types of WTA which are composed of either repetitive 1,3-glycerol-phosphate (GroP) or 1,5-ribitol-phosphate (RboP) and are modified with sugar residues and alanyl groups (Weidenmaier and Peschel 2008). Most of the *S. aureus* strains express RboP substitute with *N*-acetylglucosamine (GlcNac) and D-alanine (Xia et al. 2010; Xia and Wolz 2014).

In the environment, in order to survive, bacteria have to evolve and develop their defense mechanism against constant phage attack. However, unlike antibiotic, phage also has the ability to evolve a counter-adapt mechanism against phage-resistant bacteria. This process is called coevolution, the process that involves the adaptation and counter-adaptation of the two or more species evolve and exert selection pressure on each other. The counter-adaptation of phage against resistant host is an advantage of using phage as a therapeutic agent (Örmälä and Jalasvuori 2013).

Comprehension of the mechanisms involved and the factors affecting phage-host recognition and infection is important for phage-host interaction investigation for phage therapy candidate. This chapter describes host receptors involved in recognition and adsorption of phage ϕMR003 by adsorption assay and in silico analysis of the whole genome of the phage. Since the counter-adaptation of phage is important to investigate the success of phage therapy, this chapter also aims to investigate such characteristic of ϕMR003 with its host. I conducted a coevolution experiment of the phage with each host independently by repeated batch culturing for 5 rounds.

Next, the whole-genome of mutant phages and host were analyzed as compared with the WT strains.

4.2 Materials and methods

4.2.1 Bacterial strains and bacteriophages

S. aureus strain RN4220, *S. aureus* strain SA003 (Synnott et al. 2009) and WTA-deficient strains, including SA003ΔTarS, RN4220ΔTarM, and RN4220dTO (Table 4-1) (Azam et al. 2018) were used for the adsorption assay. The strains RN4220ΔTarS and RN4220ΔTarSTarM (Kurokawa et al. 2013) (Table 4-1) were kindly provided by Prof. Kenji Kurokawa (Nagasaki International University, Nagasaki, Japan).

Phage propagation method was conducted following the method described in section 3.2.1. MRSA strains, MR116 and MR144 were used in the coevolution with ϕMR003 that was isolated from the wastewater treatment plant. The detail characteristics of this phage are described in chapter 3. ϕSA012 and ϕSA039 were also used.

Table 4-1 Bacterial strains and phages

Strain name	Description	Reference
RN4220ΔTarM	*S. aureus* RN4220 lacking *tar*M gene	(Takeuchi et al. 2016)
RN4220ΔTarS	*S. aureus* RN4220 lacking *tar*S gene	(Kurokawa et al. 2013)
RN4220ΔTarSTarM	*S. aureus* RN4220 lacking *tar*S gene and *tar*M gene	
RN4220dTarO	*tar*O gene in *S. aureus* RN4220 was disrupted	(Azam et al. 2018)
SA003ΔTarS	*S. aureus* SA003 lacking *tar*S gene	(Azam et al. 2018)
MR116 and MR144	MRSA isolated from patients in Kyorin University Hosptital	This study

4.2.2 Efficiency of plating (EOP)

EOP was conducted based on the previously described protocol (Kutter 2009; Hyman and Abedon 2010). 10 µl of phage solution at titer 10^2, 10 and 10^{-1} PFU were spotted on the bacterial lawn and incubated for 24 h at 37°C. Next, plaques were counted on each strain and EOP was calculated by dividing PFU counts on each MRSA strains with PFU counts on control host. RN4220 was assigned as control host of ϕMR003, while SA003 was assigned as control host of ϕSA012 and ϕSA039. The EOP was classified as "High" when the ratio was equal or more than 0.5. An EOP was greater than 0.1, but below 0.5 was considered as "Medium" efficiency, and equal or lower than 0.1 was classified as "Low" efficiency (Mirzaei and Nilsson 2015). "No" was assigned when there was no plaque observed.

4.2.3 Adsorption assay

To measure the adsorption of ϕMR003 onto *S. aureus* strains, we measured free phage present in the supernatant of cell-phage contact (Takeuchi et al. 2016). *S. aureus* cells were prepared by inoculating 10% (v/v) of overnight culture into 4.5 ml of LB and incubate the diluted culture at 37 °C with 120 rpm shaking until the OD_{660} reached 1.0. Phage lysate at 10^7 PFU/ml was added into the bacterial culture. After 25 min of infection at 37 °C and 120 rpm, the bacterial culture was centrifuged at 9730 *g* for 1 min to collect the free phage and perform a plaque assay using RN4220. Either chloramphenicol or erythromycin was added into the cell culture at a concentration of 50 µg/ml, with the cell culture equilibrated for 10 min prior to infection in order to inhibit cell growth and phage development during incubation with phage (Baptista et al. 2008). Adsorption efficiency was calculated by dividing the number of adsorbed phages by the initial number of phages. A two-tailed Student's *t*-test was used to determine statistical significance.

4.2.4 Gene base analysis of WTA in MRSA

Genes *tar*O, which encode a transferase that initiates WTA synthesis, and *tar*S and *tar*M, which are glycosyltransferases of β-GlcNAc and α-GlcNAc on WTA, respectively, were detected. A prophage encoding *tar*P, which has a similar function to *tar*S and modifies the location of β-GlcNAc residue on WTA (Gerlach et al. 2018), was also detected in some MRSA strains. The 23 representative's MRSA strains were selected for detection of these four genes based on their sensitivity to ϕMR003, ϕSA012, and ϕSA039. RN4220 and SA003, were used as controls. PCR was used to amplify the four genes from genomic DNA. Overnight cultures of MRSA isolates were harvested for DNA extraction using the phenol-chloroform extraction method (Lee 2013; Ung et al. 2018). Primers used to detect the genes are listed in Table 4-2. All PCR programs were performed as following: 95 °C (5 min), 25 cycles of 95 °C (15 s), 53 °C (30 s), 68 °C (70 s for

*tar*O and *tar*M, 2 min for *tar*S, and 1 min for *tar*P) and 68 °C (5 min). The resulting amplicons were verified by electrophoresis on 1% (w/v) agarose.

Table 4-2 Primers for PCR

Primer	Sequence (5' to 3')	Reference
F_tarP	ATGAAAAAAGTAAGTGTTATAATGCCAACATTC	(Gerlach et al. 2018)
R_tarP	CTATAATAGCTTATCTGCAATCATCACAGC	(Gerlach et al. 2018)
F_tarS	GTTGACGTTTCTGACTTTAGAG	This study
R_tarS	G GCTTCTATACTTACTTGTCCGC	This study
F_tarO	AGATTCCAGCGACTATAACAG	This study
R_tarO	GCTTTAGGCTACACACATAGAC	This study
F_tarM	AATGGATCGAAGAACGAAAATGT	(Takeuchi et al. 2016)
R_tarM	CAAATATAAAAAACATTAACATAAGGCGT	(Takeuchi et al. 2016)

F: forward primer; R: reverse primer

4.2.5 In silico genome comparison of ϕMR003 and ϕSA012

Phage DNA extraction and sequencing of ϕMR003 were described in section 3.2.5. ORFs were predicted and annotated by the RAST server (Aziz et al. 2008). The genome of ϕSA012 was analyzed previously (Takeuchi et al. 2016) with accession number AB903967. Nucleotide and amino acid sequences were scanned for homologs using the Basic Local Alignment Search Tool (BLAST) (Altschup et al. 1990). Genome matcher (Ohtsubo et al. 2008) was used to visualize the comparisons between the two phage's genomes. HHpred (Söding et al. 2005) was used to predict protein function. Pairwise sequence alignments (protein) were performed with EMBOSS Stretcher (Myers and Miller 1988; Rice et al. 2000).

4.2.6 Batch-coculturing of ϕMR003 and MRSA

The coevolution between MR116 and MR144 and ϕMR003 was conducted with batch co-culture with the serial transfer. The batch co-culturing was conducted in a compact rocking incubator (TVS062CA, Advantec). Initially, 5 ml of Luria-Bertani (LB) broth in an L-shaped glass test tube was inoculated with 50 µl of an overnight culture of WT MR116 and incubated

aerobically at 37 ˚C with shaking at 40 rpm. After 1 h of incubation, approximately 10^7 CFU/ml of bacterial culture was infected with phage at a titer of 10^7 PFU/ml, MOI=1. After confirming that bacterial cells entered stationary phase (approximately 4 days of batch co-culture), 50 µl of the culture was transferred into 5 ml of fresh LB broth. Using this procedure, batch co-culture was repeated 5 times by serial transfer (Fig. 4-1).

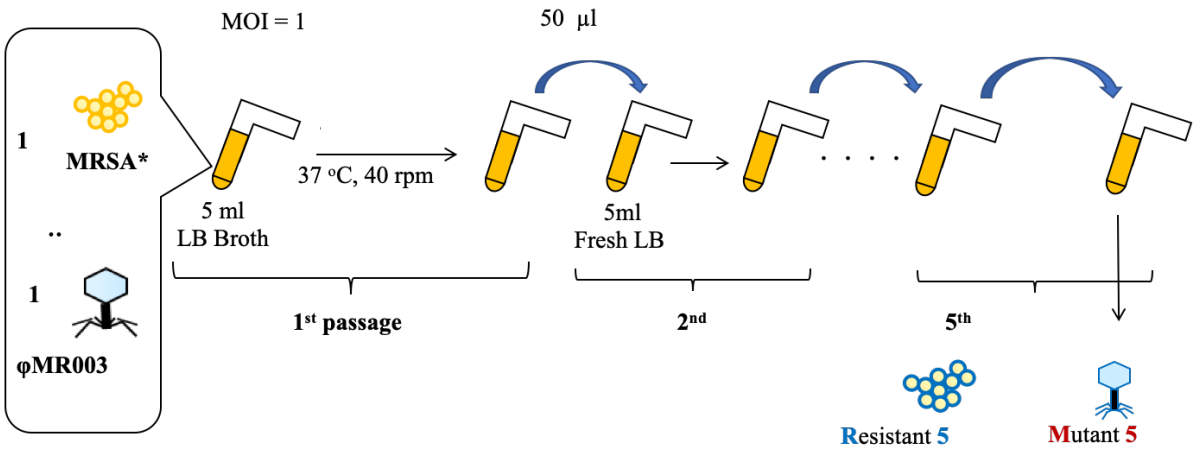

Figure 4-1 Batch co-culturing of MR116 and MR144 with ϕMR003. 5 passage of co-culturing were conducted. The culture at the final round (5th), was screened for mutant host and mutant phage.

After 5th batch culture, 2 ml of culture was centrifuged at 9730 × g for 5 min at 4 ◦C. The supernatant was used for phage genome extraction. And pellet was washed several times to remove free phage and then was used to extract the genome. The pellet of culture was used for DNA extraction using GenElute Bacterial Genomic DNA kits (Sigma, Germany). Next, the genome was submitted for their whole genome analysis by illumination Miseq at BGI (Hongkong). The whole-genome of WT host was also extracted from the overnight culture using the same method. The sequence reads were analyzed by MICRA (Caboche et al. 2017). WTA gene cluster of RN4220 (accession number: NC_007795) were searched against annotation mapped sequence generated by MICRA of the MRSA strains. The amino acid sequence alignment was conducted in EMBOSS stretcher (Myers and Miller 1988; Rice et al. 2000). The homolog sequence was searched and compared to a reference sequence by BLAST (Altschup et al. 1990). Phage genome was extracted with the same procedure in section 3.2.5 and sequence reads were assemble by Velvet ver. 1.2.10 (Zerbino and Birney 2008).

4.3 Results

4.3.1 Adsorption assay and EOP of ϕMR003

The adsorption assay and EOP were conducted to assess the adsorbed ϕMR003 and their infectivity against *S. aureus* RN4220, its mutants, as well as wild-type *S. aureus* SA003 and its mutant *S. aureus* SA003ΔTarS (Fig. 4-2a, b). The common structure of WTA of *S. aureus* was presented in Fig. 4-2c. For RN4220, adsorption of ϕMR003 was (63.2%±10.0%) which was not significant when compared to its mutants, RNΔTarM with (49.6%±3.65%) adsorbed phage (p>0.05); RNΔTarS with (71.8%±3.6%) adsorbed phage (p>0.05); RNΔTarSTarM with (52.4%±14.6%) adsorbed phage (p>0.05) (Fig. 4-2a). The EOP consistently showed high efficiency that implied successful infection of those hosts (Fig. 4-2a). However, adsorption of phage on RNdTarO was significantly lower (4.1%±6.6%) compared to RN4220 (p<0.01) (Fig. 4-2a). The EOP showed medium efficiency, implying the reduced infectivity compared to RN4220. The adsorption of phage on SA003 was 99.8%±0.1%, which was not significant to SA003ΔTarS, with adsorption of (90.7%±5.2%) (p>0.05). Although the amount of phage adsorbed on SA003 was significantly higher than the amount adsorbed on RN4220 (p<0.01), this phage inefficiently infected onto SA003 (Fig. 4-2a). Taken together, the absence of *tar*O affects the absorption of ϕMR003, but not the deletion of either *tar*S or *tar*M, or of both *tar*S and *tar*M. Nevertheless, I observed medium EOP of ϕMR003 on RNdTarO although there was a significant decrease in the amount of adsorbed phage.

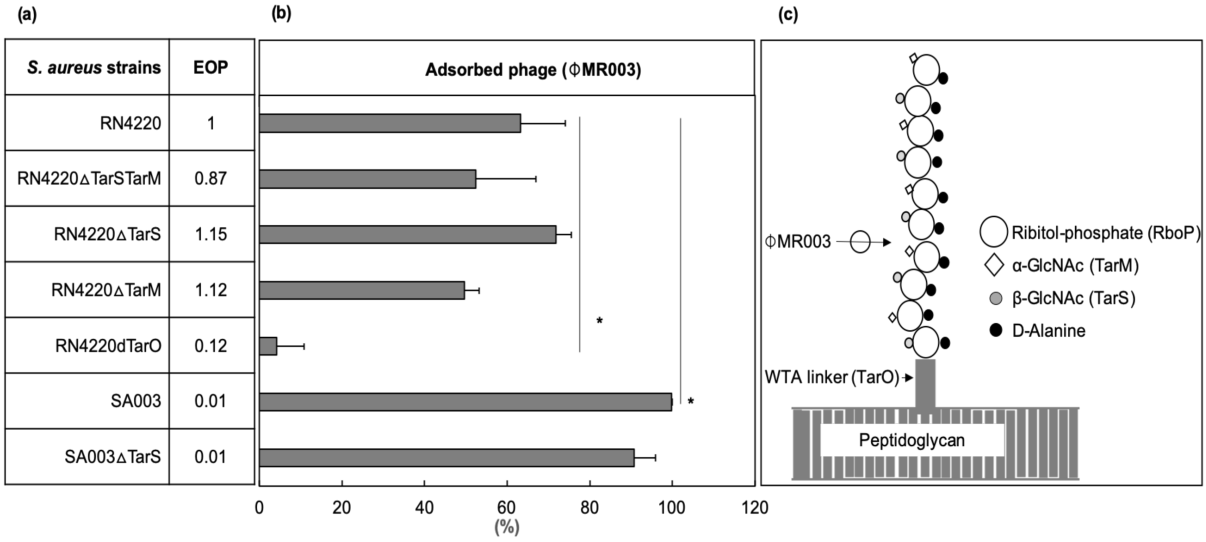

Figure 4-2 (a) EOP, (b) adsorption of ϕMR003 on *S. aureus* and (c) the common WTA structure of *S. aureus*. Data are presented as means ± standard deviations (SD, n=3). A two-tailed *t*-test was used to determine statistical significance. The arrow with a circle indicates the infectivity of ϕMR003

4.3.2 Detection of WTA gene clusters and prophage gene in MRSA

Table 4-3 shows the presence of the four genes in various *S. aureus* strains. All strains harbor *tar*O and *tar*S, with *tar*M being selective amongst strains. On the other hand, *tar*P was detected in two strains out of all sampled strains.

Table 4-3 Presence of *tar*O, *tar*S, *tar*M, and tarP of the MRSA strains and EOP

Strain	SCC*mec*	*tar*O	*tar*S	*tar*M	*tar*P	EOP		
						ϕMR003	ϕSA012	ϕSA039
RN4220	n/a	○	○	○	x	1.0 (H)	0.1 (L)	< 0.1 (L)
SA003	n/a	○	○	x	x	0.2 (M)	1.0 (H)	1.0 (H)
MR003	II	○	○	x	x	0.7 (H)	0.4 (M)	0.8 (H)
MR005	II	○	○	x	x	1.3 (H)	0.7 (H)	0.7 (H)
MR022	IV	○	○	○	x	0.9 (H)	0.5 (H)	0.6 (H)
MR039	IV	○	○	○	x	1.6 (H)	0.8 (H)	0.8 (H)
MR045	IV	○	○	○	x	1.4 (H)	0.6 (H)	0.7 (H)
MR053	II	○	○	x	x	0.7 (H)	0.4 (M)	0.5 (H)
MR057	II	○	○	x	x	1.8 (H)	0.3 (M)	0.2 (M)
MR102	IV	○	○	○	x	0.6 (H)	0.7 (H)	0.3 (M)
MR116	IV	○	○	○	x	1.2 (H)	0.3 (M)	0.3 (M)
MR035	I	○	○	○	x	0.8 (H)	0.3 (M)	(N)
MR050	I	○	○	○	○	0.8 (H)	0.6 (H)	(N)
MR054	IV	○	○	○	x	1.2 (H)	0.3 (M)	(N)
MR113	II	○	○	x	○	1.3 (H)	0.7 (H)	0.1 (L)
MR121	IV	○	○	○	x	1.4 (H)	0.3 (M)	(N)
MR124	IV	○	○	○	x	0.9 (H)	0.3 (M)	(N)
MR009	IV	○	○	○	x	0.7 (H)	(N)	(N)
MR049	IV	○	○	○	x	0.9 (H)	0.1 (L)	(N)
MR051	II	○	○	x	x	0.5 (H)	0.1 (L)	< 0.1 (L)
MR108	IV	○	○	○	x	0.5 (H)	< 0.1 (L)	(N)
MR144	IV	○	○	○	x	0.9 (H)	0.1 (L)	(N)
MR058	IV	○	○	○	x	(N)	(N)	(N)
MR132	IV	○	○	x	x	(N)	0.5 (H)	0.2 (M)

EOP was determined as a ratio of PFU on MRSA strains versus PFU on control strains. RN4220 was a primary host and used as the control strain for ϕMR003. SA003 was a primary host and used as the control strain for ϕSA012 and ϕSA039. EOP ≥ 0.5 defined as High (H); 0.1

< EOP < 0.5 defined as Medium (M); EOP ≤ 0.1 defined as Low (L); No plaque observed (N). (○) detected; (x) not detected

The presence of tarO genes in MRSA strains were not correlate to the infection of the three phages based on EOP. Other genes involved in WTA synthesis between RN4220 and SA003 were compared using their whole genome (genome accession number: NC_007795 and AP018376, respectively) (Nair et al. 2011; Azam et al. 2018). Since WTA is the main receptor for ϕMR003 adsorption, the key enzyme involved in WTA synthesis of SA003 and RN4220 was hypotheses to be different because of the different EOP of ϕMR003 to both hosts. The amino acid sequences of key enzymes of WTA synthesis between both hosts were aligned. However, the sequence of *tar*O of RN4220 and SA003 was 100% identical while *tar*S showed 99% identity. *tar*M was absent in SA003, however, the absence of *tar*M did not affect the infection of ϕMR003 into the host cell.

4.3.3 Putative tail and base plate proteins ϕMR003

In chapter 3, ϕSA012 and ϕMR003 showed different host specificities against MRSA strains. Since RBPs play an important role in host range specificities, I hypothesized that ϕSA012 and ϕMR003 possess different RBPs. In this chapter, the putative RBPs of both phages (Fig. 4-3a) were compared.

A previous study described *orf103* and *orf105* of ϕSA012 as encoding RBPs against *S. aureus* (Takeuchi et al. 2016). The homologous to *orf103* and *orf105* of ϕSA012 were searched in ϕMR003 genome by BLAST (Fig. 4-3a). ORF103 of ϕSA012 contains 640 amino acids, whereas its homolog, ORF117 in ϕMR003, contains 637 amino acids with about 75% amino acid identity. In addition, 72% of amino acid identity was observed between *orf105* in ϕSA012 and its homolog *orf*119 in ϕMR003.

Other regions encoding putative tail and baseplate proteins (Fig. 4-3b) between ϕSA012 and ϕMR003 were investigated. Most of them showed amino acid similarities under 85%. *orf*89 of ϕSA012 was homologous to a split region (*orf103*, 104, and 105) in ϕMR003. *orf103* and *orf105* showed a higher similarity of amino acid alignment than that of *orf*104 in ϕMR003 to *orf*89 in ϕSA012 (Fig. 4-3b). *orf*89 of ϕSA012 encoded putative phage lysin which is similar to *orf103* and *orf105* of ϕMR003. In addition, *orf*104 of ϕMR003 encodes an *N*-acetylglucosaminidase motif based on HHpred (protein motif prediction). Located primarily within the phage tail, this enzyme's function is to hydrolyze peptidoglycan which facilitates phage genome entry into host

cells (Moak and Molineux 2004; Xiang et al. 2008). So, the differences in tail and baseplate protein of ϕMR003 and ϕSA012 contribute to their different host specificities.

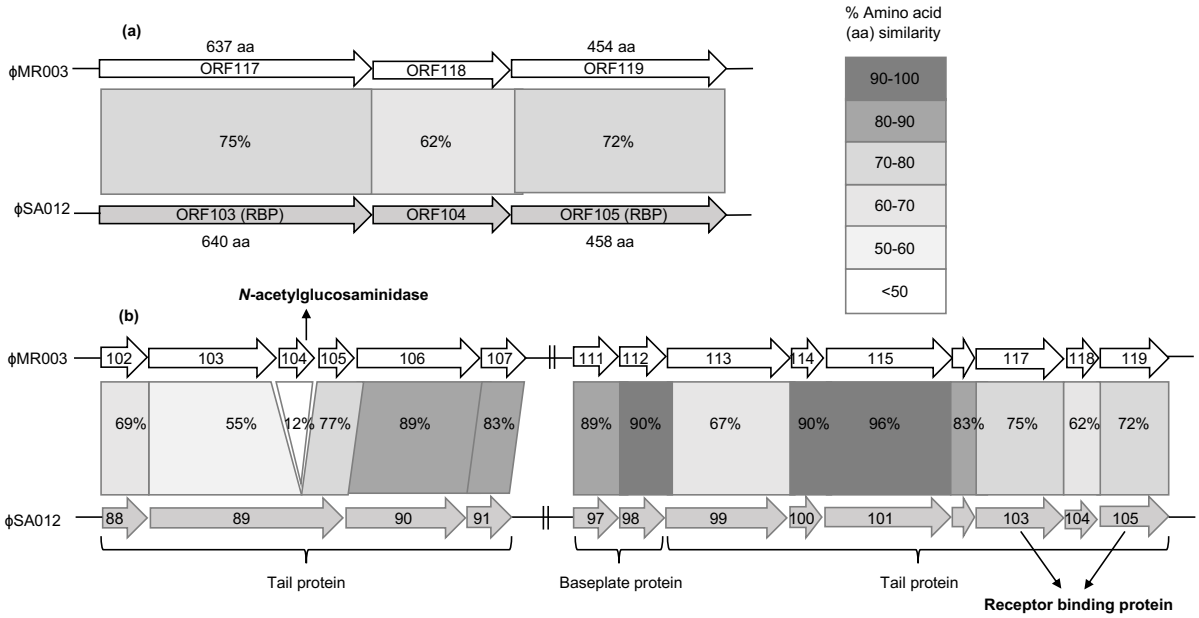

Figure 4-3 (a) Comparison of the RBPs and (b) putative tail and baseplate protein of ϕMR003 and ϕSA012

4.3.4 Genomic analysis of mutant phages ϕMR003

The whole-genome of WT ϕMR003 was revealed in chapter 3. ϕMR003 contains a double-stranded DNA comprising 132,152 bp with 185 putative predicted ORFs and 30% GC content. Based on whole genome comparison within phage database and the morphology observation, ϕMR003 belongs to the genus *Silviavirus* of *Herelleviridae* family.

After five passage of batch culturing of ϕMR003 with either MR116 or MR144, mutant phage was isolated. The supernatant obtained from the batch culture was used to perform a plaque assay with RN4220. Next, the single plaque was pick and purified followed by DNA extraction and sequencing. The sequence reads of mutant phages were mapped against WT phage so that point mutation was extracted. In mutant phage, ϕMR003/R5-MR116 (mutant phage isolated from round 5 under coevolution of ϕMR003 and MR116), mutations were found in 2 ORFs (*orf*117 and *orf*95). While the ϕMR003/R5-MR144 (mutant phage isolated from round 5 under coevolution of ϕMR003 and MR144), mutations were found in 3 ORFs (*orf*117, *orf*114, and *orf*134) (Table 4-4). The *orf*117, *orf*95, *orf*114, *orf*134 are located on the tail of the phage.

Table 4-4 Mutations in mutant ϕMR003 during coevolution with MRSA strain

ORF (ϕMR003)	Amino acid alternation	
	ϕMR003 → ϕMR003/R5-MR116	ϕMR003 → ϕMR003/R5-MR144
117	GAT (D) → AAT (N)	AGA (R) → ATA (I)
	GTA (V) → GCA (A)	GAA (E) → AAA (K)
		GAT (D) → AAT (N)
95	GAT (D) → AAT (N)	x
114	x	AAA (K) → AAC (N)
134	x	GGT (G) → GAT (D)

x: absent

4.3.5 Identification of mutations in WTA gene

Sequence reads of WT and mutant host were analyzed. Genes *tar*O, *tar*S, and *tar*M which are involved in WTA synthesis were compared between WT and mutant host. Gene *tar*S of mutant R5-MR116 acquired 1 mutation. While gene *tar*S in mutant host R5-MR144 acquired 8-point mutations (Table 4-5).

Table 4-5 Point mutation in the mutant host during coevolution

WTA genes	Amino acid alternation between WT and mutant host	
	WT → R5-MR116	WT → R5-MR144
*tar*S	GAT (D) → AAT (N)	GAT (D) → AAT (N) ACA (T) → GCA (A) GAT (D) → AAT (N) GAA (E) →AAA (K) ATT (I) → GTG (V) GAA (E) → CAA (Q) ATG (M) → ATC (I) TCG (S) → CCA (P)

4.4 Discussions

4.4.1 ϕMR003 requires WTA for adsorption

The deletion of *tar*O resulted in the deletion of a whole set of WTA from RN4220, leading to a significant decrease of adsorption by ϕMR003 into the host (Fig. 4-2b). Deletion of glycosyltransferase TarM and TarS resulted in the deletion of α-GlcNAc and β-GlcNAc residues on WTA, respectively, but this modification did not affect the ability of ϕMR003 to adsorb on to the host (Fig. 4-2b). These results imply that ϕMR003 requires backbone of WTA as its host receptor which is consistent with most phages of the *Herelleviridae* family, including ϕSA012 (Azam et al. 2018), phage K, and ϕ812 (Xia et al. 2011). Nevertheless, ϕSA039 which is in the same family was recently reported to utilize both backbone and β-GlcNAc residues on WTA as its host receptor (Azam et al. 2018).

WTA is conserved in all of the *S. aureus* strains because it is important for cell division (Winstel et al. 2014). The presence of *tar*O gene was consistently detected, indicating the presence of WTA in all of the selected MRSA (Table 4-3). The presence of WTA on the cell surface of MRSA strains could support ϕMR003 infection and thus promote the wide host range of this phage. MR132 and MR58 harbor *tar*O (Table 4-3). However, MR132 showed resistance to ϕMR003 and susceptibility to ϕSA012 and ϕSA039, whereas MR58 showed resistance to all three phages. Phage-resistant mechanisms involve the restriction-modification (R-M) system in bacteria (Azam and Tanji 2019b). The Sau3AI restriction enzyme is present in some *S. aureus,* which targets GATC sites in the viral genome. In contrast to phage K, ϕSA012, and ϕSA039, the genome of ϕMR003 has a Sau3AI restriction site (GATC) which may influence the infectivity of the phage against *S. aureus* harboring Sau3AI. The clonal complex of MRSA has a different R-M system which inhibits horizontal gene transfer from one clonal complex to another and overcomes phage attack (Roberts et al. 2013). The R-M system of MR58 may contribute to the insensitivity to ϕMR003, ϕSA012, and ϕSA039. Therefore, whole genome data from MR132 and MR58 would be essential for future studies. Although a high adsorption activity of ϕMR003 on SA003 was observed, the infectivity of ϕMR003 against SA003 was low (Fig. 4-2a, b). Based on whole genome analysis in SA003, the R-M system of type I were detected with some of them absent in RN4220. This R-M may influence the infectivity of ϕMR003 against SA003.

4.4.2 In silico analysis of ϕMR003 reveals potential viral proteins contributing to wide host range

Although ϕSA012 infection requires WTA on the host cell surface, this phage shows a narrow host range to MRSA compared to ϕMR003. The difference in baseplate and tail proteins could be a key factor in the difference in their host specificities. *Orf*117 and *orf*119 of ϕMR003 showed identity (75% and 72%) to the homologous region (*orf103* and *orf105*) of ϕSA012. RBPs (ORF103 and ORF105) of ϕSA012 recognized different components of WTA for host adsorption.

RBP (ORF103) of ϕSA012 binds to α-GlcNAc residues of RboP-WTA, whereas, RBP (ORF105) binds to the WTA backbone of *S. aureus* (Takeuchi et al. 2016). The functional protein encoded by *orf*119 of ϕMR003 may also bind to the WTA backbone because the entire region of the protein encoded by this ORF, which includes a PHA01818 domain, is similar to the RBP-encoding *orf105* of ϕSA012. In contrast, in *orf*117 of ϕMR003, a PHA01818 domain is located in the C-terminus, similar to the RBP-encoding *orf103* of ϕSA012. The PHA01818 domain is conserved in the hypothetical proteins of staphylococcal lytic phages that belong to the genus *Kayvirus* (Uchiyama et al. 2014b). The function of the PHA01818 domain remains unknown but this domain could be associated with phage adsorption activity (Uchiyama et al. 2014a; Takeuchi et al. 2016). The functional protein encoded by *orf*117 of ϕMR003 possesses a carbohydrate binding domain motif that is similar to phage K (59% amino acid identity). The RBP encoding ORF103 of ϕSA012 also has a similar carbohydrate binding domain to that of phage K (99% amino acid identity) which recognizes different sites on WTA compared with RBP ORF105 (Takeuchi et al. 2016). Thus, the functional protein encoded by *orf*117 could bind to another component on WTA different from that of the functional protein encoded by *orf*119.

According to a previous study, ϕSA012 is closely related to ϕSA039, but they have distinct host specificities. ϕSA039 requires backbone and β-GlcNAc residues of WTA, but ϕSA012 only requires the backbone of WTA. The baseplate and tail proteins of both phages show a similar level of identity (83–88%) which contributes to the difference in host specificity between them (Takeuchi et al. 2016; Azam et al. 2018). The low amino acid alignment between the RBP-encoding genes of ϕSA012 (*orf103* and *orf105*) to homologous regions in the ϕMR003 genome (*orf117* and *orf119*) may contribute to the difference in host specificity.

The *orf104* encodes *N*-acetylglucosaminidase (glucosaminidase domain) presents in the gene encoding phage tail fiber of ϕMR003 and absent in ϕSA012, although this ORF had a low identity to C-terminal of ORF89 in ϕSA012 (12% identity). *N*-acetylglucosaminidase is one of many VALs that hydrolyze glycosidic crosslinks between alternating *N*-acetylglucosamine and *N*-acetylmuramic acid residues that make the peptidoglycan lattice of bacterial cell walls. Several types and functions of VALs were reviewed elsewhere (Fernandes and São-José 2018). Each VAL cleaves specific peptidoglycan bonds. During the phage infection cycle, the phage needs to degrade the host cell envelope for entry with the support of the enzymes produced by the phage itself (Fernandes and São-José 2018). Gram-positive bacterial cell walls contain a thick peptidoglycan layer. In *S. aureus*, penicillin-binding protein 4 is a nonessential transpeptidase that is required for high levels of peptidoglycan crosslinking (Loskill et al. 2014). This protein is essential for β-lactam resistance in CA-MRSA. The presence of *N*-acetylglucosaminidase in the

tail of ϕMR003 may facilitate penetration of the phage genome into *S. aureus* host cell with either normal or high levels of peptidoglycan crosslinking. The C-terminal of gp49 (located in baseplate) of phage ϕ11 encodes a peptidoglycan degrading enzyme (glucosaminidase domain) that is similar to functional protein encoded in ORF104 of ϕMR003. The presence of this enzyme in ϕ11 support host lysis. Deletion of gp49 results in the delay of host lysis (Rodríguez-Rubio et al. 2013).

Moreover, in the disruption of *tar*O in RN4220, although ϕMR003 showed low adsorption activity, the EOP result showed medium efficacy (slightly infect) (Fig. 4-2). But ϕSA012 cannot infect RN4220dTarO (Azam et al. 2018). VALs produced by ϕMR003 encoded in ORF104 may facilitate the infection of ϕMR003 onto WTA-null RN4220. A depolymerase has also been reported to show the peptidoglycan hydrolysis motif (Pires et al. 2016). Depolymerase is involved in the degradation of biofilms by *S. aureus*, and some strains of MRSA usually appear as biofilms (Paharik and Horswill 2016). Therefore, the difference in the baseplate and tail protein and the presence of *orf104*, which encodes peptidoglycan hydrolase in ϕMR003, helps promote a wider host range against MRSA compared with ϕSA012.

4.4.3 Prophage-encoded *tar*P in MRSA confers resistance to ϕSA039

Although the *tar*S gene, which encodes β-GlcNAc transferase, was detected in all representative MRSA strains, ϕSA039 did not infect all of them. TarP protein, which was recently reported to be a prophage-encoded protein in MRSA strains, can translocate β-GlcNAc residues in WTA, and inhibit infection by β-GlcNAc targeting phage, e.g., *Podoviridae* phage (Gerlach et al. 2018). In this aspect, the presence of TarP protein in MRSA may confer resistance to ϕSA039. I detected the *tar*P gene in MR050 and MR113 with no plaque observed and low EOP, respectively (Table 4-3). Although gene *tar*P was not detected in other MRSA strains because of either limited primer specificity or the absence of *tar*P, it may suggest that *tar*P is one of the limiting factors in using β-GlcNAc-targeting phage on MRSA.

The gene of *tar*P was not detected in the ϕMR003 genome. Thus, the transfer of this gene to MRSA is unlikely to occur, making this phage safer to use for therapeutic purposes. Moreover, since the backbone of WTA is essential for infection by ϕMR003, I can expect promising results in its use in phage therapy.

4.4.4 ϕMR003 acquired the spontaneous mutations in RBP during coevolution

In silico analysis of ϕMR003 and its mutant phages shows that all of the mutations were linked to RBP and genes encoding tail protein. The *orf117* is a putative RBP which is homolog to *orf103* and *orf100* of ϕSA012 and of ϕSA039, respectively.

In the previous study, ϕSA012 and of ϕSA039 harbored 2 RBPs which are responsible for their wide host range against *S. aureus.* ϕMR003 encodes 2 homologs RBPs (encoded in ORF117 and ORF119) to the RBPs (encoded in ORF103 and ORF105) of ϕSA012 and to the RBPs (encoded in ORF100 and ORF102) of ϕSA039. The mechanism of phage-resistant in bacteria involves several factors such as inhibition of phage adsorption by altering the phage receptor. For example, in *S. aureus* SA003 removes a β-GlcNAc residue on the WTA to prevent adsorption of the specific phages ϕSA039. As a counter-adaptation, phages can adapt to changes in a receptor by acquiring a point mutation in its gene of RBPs (Azam et al. 2018). ϕSA039 requires backbone of WTA and β-GlcNAc. The removal of the gene encoding β-GlcNAc from WTA inhibit the infectivity of ϕSA039. Mutation in *orf100* of ϕSA039 enables this phage to infect SA003 lacking β-GlcNAc (Azam et al. 2018). During the coevolution, mutations in *orf103* of ϕSA012 inhibit the infectivity of ϕSA012 on RN4220. While deletion of *tar*M which results in deletion of α-GlcNAc of the WTA, enable infectivity of ϕSA012 (Takeuchi et al. 2016).

During the coevolution with its host, ϕMR003 mutated in RBP ORF117 and other genes encoding phage tail proteins. In mutant host, spontaneous mutations were observed in *tar*S gene encoding β-GlcNAc transferase on WTA. So, the alteration of *tar*S is linked to the counter-adaptation of mutant ϕMR003.

CHAPTER 5 Synergistic effects of ϕMR003 and antibiotic on control of MRSA

5.1 Introduction

The inability to treat MRSA is a major clinical challenge. This has been caused by the ability of MRSA strains to be tolerance to antibiotic and resistant to multiple antibiotic classes (Kumaran et al. 2018). Phage therapy has been proposed as a promising alternative to antibiotics, but some studies suggested that phage is similar to antibiotic when using alone, it can create a selection pressure for resistant strain emergence either in vitro or in vivo (Osada et al. 2017; Azam et al. 2018; Azam and Tanji 2019b). In this aspect, combined therapy has been proposed to provide better treatment outcome than single therapy (Torres-Barcel and Hochberg 2016).

In this chapter, I describe synergistic effects of ϕMR003 and antibiotic on controlling of MRSA strain. Different treatment conditions were analyzed including single treatment and combined treatment of the different administration time of ϕMR003 or antibiotic.

5.2 Materials and methods

5.2.1 Bacterial strains, bacteriophage, and culture conditions

ϕMR003 infection of representative MRSA strain MR116 was assessed in vitro for 72 h. Briefly, 50 µl of bacterial overnight culture was inoculated into 5 ml of LB and incubated for 1 h prior to either phage infection or antibiotic addition in a TVS062CA BioPhoto recorder (Advantec, Tokyo, Japan), with the optical density at 660 nm (OD_{660}) measured every 15 min. Under all experimental conditions, the bacterial cell concentration was adjusted to 10^7 CFU/ml, while phage concentration was 10^7 PFU/ml (MOI of 1). Oxacillin (Wako, Japan) which is a common antibiotic used to treat *S. aureus* infection, was used at 5 µg/ml, either alone or in combination with phage either added simultaneously or in sequence. After incubating the bacterial culture for 1 h, either phage (P) or oxacillin (O) was added. For simultaneous combination treatment, oxacillin and phage were added at the same time at 1 h (M). In sequential combination treatment, oxacillin was added at 1 h followed by phage at 3 h (OP), or else phage added at 1h followed by oxacillin at 3h (PO). Bacterial cultures without phage or antibiotic added were conducted as controls.

Bacterial cell and phage were enumerated at 24 h, 48 h, and 72 h. Bacterial CFU and phage PFU counts were $\log_{10}$ transformed. The interaction of synergy, additive or antagonistic of

combination treatments of phage and antibiotic against *S. aureus* were determined according to the previous study (Kumaran et al. 2018). The interaction was defined as being synergy if the combination treatments resulted in greater bacterial reduction than the sum of the individual treatments. And as being additive if bacterial reductions in combination treatments equal to the sum of the individual effects. While an antagonistic if the bacterial reduction in combination treatments were lower than the sum of individual effects. A two-tailed Student's *t*-test was used to determine statistical significance between bacterial reduction in combination treatments and the sum of the individual phage and antibiotic treatment.

5.3 Results

Growth curves of MR116 in the presence of either ϕMR003 (P), oxacillin (O), or both ϕMR003 and oxacillin adding at the same time (M), oxacillin first followed by phage (OP), and phage first followed by oxacillin (PO) are presented in Fig. 5-1. In (O)-treated MR116, although the maximum OD_{660} of MR116 was lower than that of the control culture by almost half, OD_{660} did not decline, which indicated that oxacillin was ineffective against MR116. Unlike (O) treatment, in (P) and (PO) treatment, a decline in OD_{660} due to cell lysis was observed after 3 h. During (M) and (OP) treatment, OD_{660} declined after about 7 h. Under these conditions, prior to bacterial lysis, a high bacterial growth peak was observed. Among all, the peaks observed during (P) and (PO) treatment were the lowest, indicating high bacterial fragmentation. However, at around 18 h of (P) treatment, phage-resistant bacteria appeared (Fig. 5-1). Counteradaptation of host and phage was observed at around 25 h in (OP) and (M) and 35 h in (PO) (Fig. 5-1).

The observation of OD_{660} did not reflect the actual viable cell. So, the viable cell was count. And the synergistic effects were calculated based on the viable cell. (M) and (OP) treatments resulted in synergy interaction (24 h to 72 h) because the bacterial reduction in the combined treatments was greater than the sum of the individual phage and oxacillin ($p< 0.05$) (Fig.5-2). In (PO) treatment, synergy interaction was observed within 24 h to 48 h. But the additive interaction was observed at 72 h because the bacterial reduction was greater yet not significantly different ($p>0.05$) than the sum of the individual treatment (Kumaran et al. 2018). Viable density in (M) and (PO) increased around 1 to 3 logs, respectively between 24 h to 72 h. However, cell density in (OP) decreased around 2 logs between 24 h to 72 h. Cell density in control, (O) and (P) were decreased around 1 log from 24 h to 48 h and almost stable till 72 h (Fig. 5-2). The phage concentration in single phage and combination treatment were increased in relative to the initial inoculation concentration (Fig. 5-3). However, in (P) and (PO) treatment, phage concentrations were higher than in (M) and (PO) at 24 h. Phage concentration in (P) was decreased around 1 to

2 logs at 48 h and 72 h, respectively. While, in (PO), the titer was decreased around 1 log at 48 h and 72 h. Phage titer in (M), (OP) were relatively stable within the treatment period.

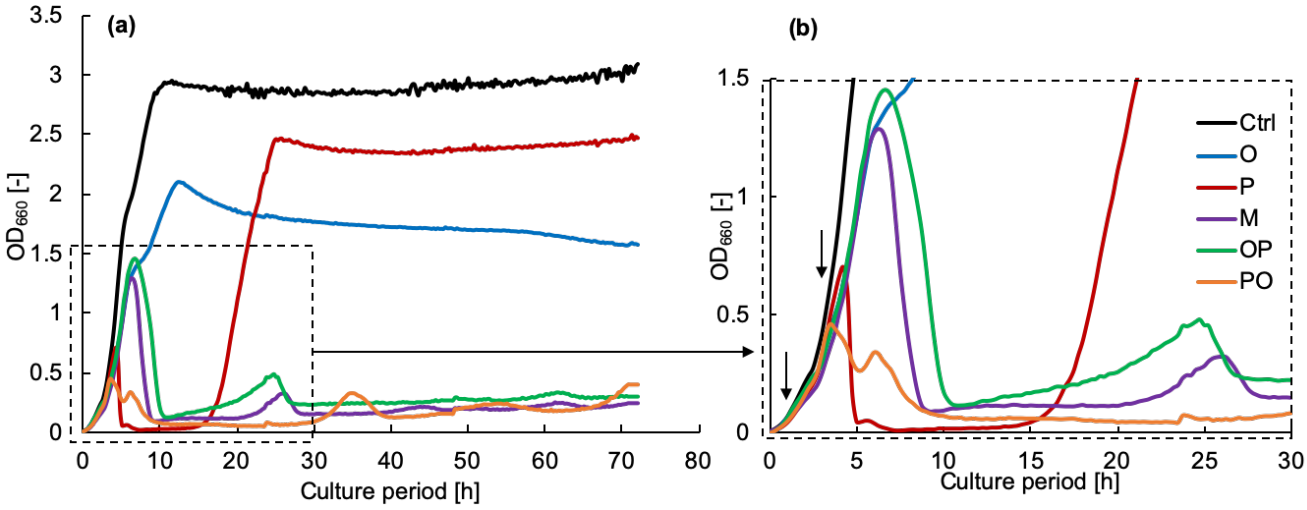

Figure 5-1 Killing curves of MR116 treated with ϕMR003 and oxacillin. P: single phage treatment; O: 5 μg/ml oxacillin treatment; M: phage and oxacillin were added simultaneously at 1 h; OP: oxacillin was added after 1 hour followed by phage at 3 h; PO: phage was added after 1 hour followed by oxacillin at 3 h. Arrow indicates the time of ϕMR003 and/or oxacillin addition.

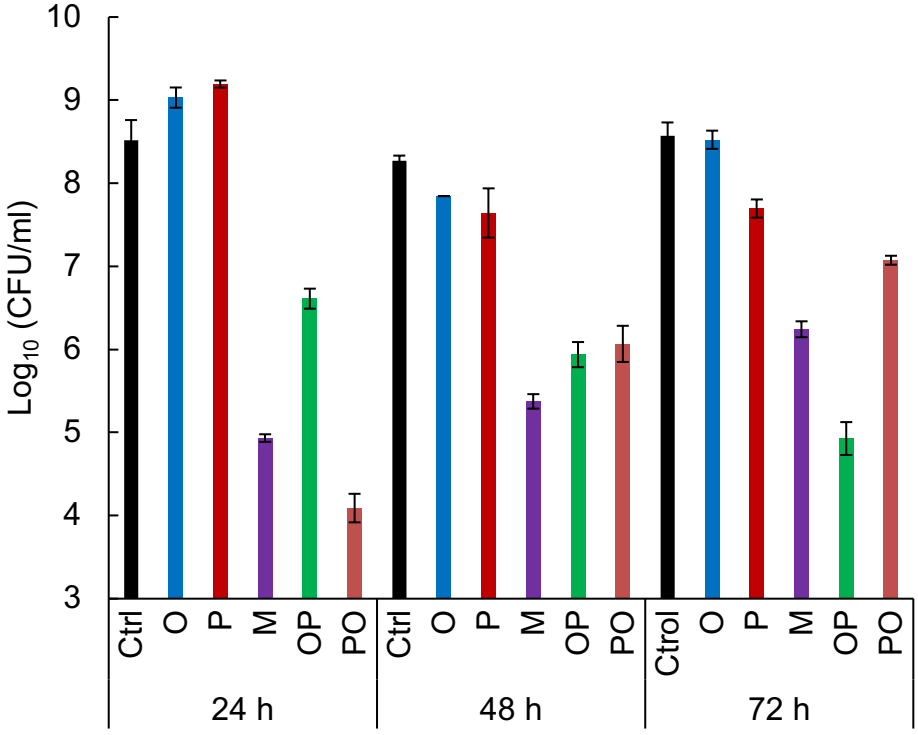

Figure 5-2 Viable count of MR116 in ϕMR003 and/or oxacillin treatment

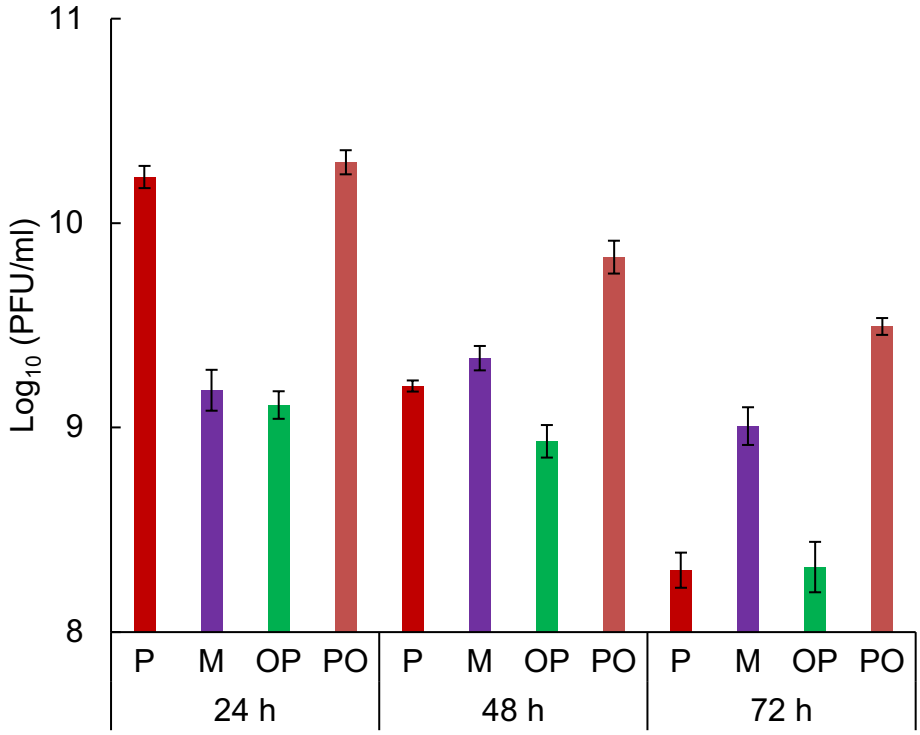

Figure 5-3 Titers of ϕMR003 in single or combination treatment

5.4 Discussions

In the current study, the combination effects of ϕMR003 and oxacillin in comparison to single ϕMR003 or oxacillin treatment in controlling MRSA (MR116) in vitro were assessed. MR116 harbored SCC*mec* IV that conferred resistant to oxacillin. In the present of oxacillin, MR116 paid much cost for growing with OD_{660} max was lower than that of control culture (Fig.5-1). With the dual effect of oxacillin and phage, the synergistic effects were observed in the combination treatment.

In the short treatment at 24 h, (PO) gave better cell reduction because of the rapid lysis of the phage followed by oxacillin treatment (Fig. 5-1, Fig. 5-2). The curve of (M) and (OP) showed relatively similar trend, time of cell lysis and phage host counteradaptation (peak) (Fig. 5-1). However, the addition of oxacillin and phage at the same time (M) gave a greater effect that the addition of phage after oxacillin (OP) for short treatment period (24 h) (Fig. 5-2). Cell continued to grow in relative to a prolonged treatment period in (M). While in (OP), cell decreased (Fig. 5-2). The result implies that synergy interaction was observed in combination treatment yet it depended on the duration of the treatment. Previous studies also observed the synergy interaction of the combination treatments of phage and antibiotics (Chaudhry et al. 2017; Kumaran et al. 2018). I observed that between 10 h to 15 h, all conditions except control and (O), decreased of

OD were observed. The OD decreased implies lower cell concentration. From that point of view, either single phage or combination, the efficacy was observed. However, in the prolonged treatment, it allowed the selection of mutants bacterial so that single phage treatment alone may be not sufficient (Osada et al. 2017).

Nevertheless, our study is limited to in vitro study, therefore further observation in vivo experiment would be essential and may give a different outcome. The success of phage therapy in vivo was reviewed recently (Azam and Tanji 2019a) as well as the combined effects of phage and antibiotics (Tagliaferri et al. 2019).

CHAPTER 6 Conclusion and perspectives

MRSA is one of the biggest current threat to global health. An increasing number of its infections are becoming harder to treat resulting in a high mortality rate. The acquisition of antibiotic-resistant in MRSA is not only through horizontal gene transfer but also by spontaneous mutation. In chapter 2, I found that through stepwise batch culturing of *S. aureus* with oxacillin, the sensitive *S. aureus* strain developed into the resistant strain. Based on in silico analysis between the genome of WT strain and the mutant strains, several point mutations were found such as in PBP4 in strain C4 (*S. aureus* resistant to 4 μg/ml of oxacillin). The PBP4 is one of the key enzymes involves in peptidoglycan crosslink synthesis. Since oxacillin targets PBPs, thus mutation in this gene interfere with the binding of oxacillin, so the strain can survive under oxacillin treatment. I also found a mutation in *yvq*F gene in strain C4, strain C800, and strain C1600. This gene encoding protein plays as a cell wall stimulant active antibiotic response and help in repairing the damaged cell wall caused by the antibiotic action in *S. aureus*.

The therapeutic agent such as phage is a suitable strategy to combat MRSA. Phage which is strictly lytic and possesses a broad host range is an ideal phage therapy candidate. In chapter 3, ϕMR003 was isolated from influent of a municipal wastewater treatment plant in Tokyo and this phage possesses a broad host range against MRSA of human origin. ϕMR003 infected 97% of MRSA strains that originated from humans (i.e. 101 out of 104 MRSA strains screened in Kyorin University Hospital). In contrast, *Kayvirus* phages, ϕSA012 and ϕSA039 (previously isolated from influent of a wastewater treatment plant and have a broad host range against bovine mastitis *S. aureus*) infected 73% and 57% of human origin MRSA. Based on the whole-genome analysis and comparison to the phage database, ϕMR003 belongs to the genus *Silviavirus* which has not been studied extensively. So, ϕMR003 is considered a potential phage therapy candidate for MRSA infections.

ϕMR003 recognizes and bind to WTA which is the most abundant molecule on the outer layer of *S. aureus* cell wall. In silico comparisons of the genomes of ϕMR003 and ϕSA012 revealed that ORF117 and ORF119 of ϕMR003 are homologs to the RBPs, ORF103 and ORF105 of ϕSA012, with amino acid similarities of 75% and 72%, respectively. Moreover, the differences in tail and baseplate proteins of both phages were detected which are key contributing factors to the different host specificities of ϕMR003 and ϕSA012. In the tail of ϕMR003 possess a unique gene encoding *N*-acetylglucosaminidase (glucosaminidase domain which hydrolyzes the peptidoglycan) which may facilitate the infection of ϕMR003 on WTA-null *S. aureus*.

Unlike antibiotic, phage has the ability to counter-adapt toward the mutant host. That is one of the advantages of phage therapy. In chapter 4, I found that during the coevolution between ϕMR003 and its host, the spontaneous mutation in mutant ϕMR003 and mutant host were observed. The mutations were observed in *orf117* of ϕMR003 which encodes the RBP. While in the mutant host, *tar*S gene encoding β-GlcNAc of the WTA. It implies the importance of RBP ORF117 in counteracting with its mutant host during the coevolution.

Fig 6-1 shows the host recognition (adsorptivity) of ϕMR003, ϕSA012, and ϕSA039 on modified RboP type WTA.

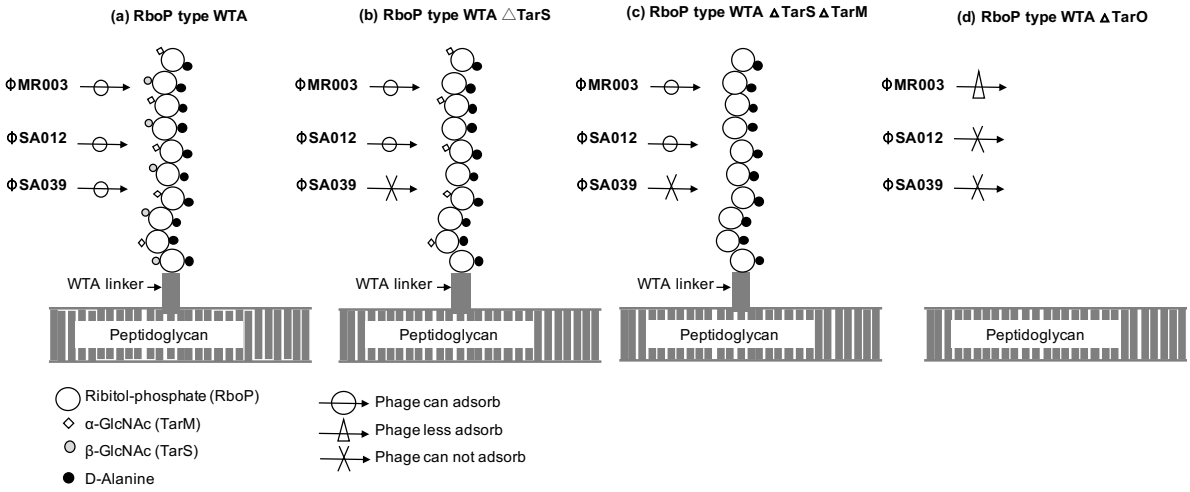

Figure 6-1 The adsorption of ϕMR003, ϕSA012, and ϕSA039 on WTA-deficient *S. aureus*

The drawback of using a single antibiotic or phage is the selection of resistant strains. In order to overcome this, combination treatments suggested being more effective than the single treatment. In chapter 5, ϕMR003 was combined with oxacillin and found to give a synergistic effect on controlling of MRSA strains in vitro. The synergistic effects were dependent on the period and conditions of the treatment. Therefore, optimization of the combined therapy is crucial before applying it into clinical practice. Moreover, as the future study in vivo of ϕMR003's therapy on MRSA infection is essential to better understand the potential of ϕMR003 as a phage therapy candidate.

7 References

Adriaenssens EM, Rodney Brister J (2017) How to name and classify your phage: an informal guide. Viruses 9:1–9 . doi: 10.3390/v9040070

Altschup SF, Gish W, Miller W, Myers EW, Lipman DJ (1990) Basic local alignment search tool. J Mol Biol 215:403–410 . doi: 0.1016/S0022-2836(05)80360-2

Azam AH, Hoshiga F, Takeuchi I, Miyanaga K, Tanji Y (2018) Analysis of phage resistance in *Staphylococcus aureus* SA003 reveals different binding mechanisms for the closely related twort-like phages ϕ SA012 and ϕ SA039. Appl Microbiol Biotechnol 102:8963–8977 . doi: 10.1007/s00253-018-9269-x

Azam AH, Tanji Y (2019a) Peculiarities of *Staphylococcus aureus* phages and their possible application in phage therapy. Appl Microbiol Biotechnol 103:4279–4289 . doi: 10.1007/s00253-019-09810-2

Azam AH, Tanji Y (2019b) Bacteriophage-host arm race : an update on the mechanism of phage resistance in bacteria and revenge of the phage with the perspective for phage therapy. Appl Microbiol Biotechnol 103:2121–2131 . doi: 10.1007/s00253-019-09629-x

Aziz RK, Bartels D, Best AA, DeJongh M, Disz T, Edwards RA, Formsma K, Gerdes S, Glass EM, Kubal M, Meyer F, Olsen GJ, Olson R, Osterman AL, Overbeek RA, McNeil LK, Paarmann D, Paczian T, Parrello B, Pusch GD, Reich C, Stevens R, Vassieva O, Vonstein V, Wilke A, Zagnitko O (2008) The RAST server: rapid annotations using subsystems technology. BMC Genomics 9:75 . doi: 10.1186/1471-2164-9-75

Bal AM, Gould IM (2005) Antibiotic resistance in *Staphylococcus aureus* and its therapy. Pharmacotherapy 6:2257–2269 . doi: 10.1517/14656566.6.13.2257

Baptista C, Santos MA, São-José C (2008) Phage SPP1 reversible adsorption to *Bacillus subtilis* cell wall teichoic acids accelerates virus recognition of membrane receptor YueB. J Bacteriol 190:4989–4996 . doi: 10.1128/JB.00349-08

Boyle-Vavra S, Yin S, Jo DS, Montgomery CP, Daum RS (2013) VraT/YvqF is required for methicillin resistance and activation of the VraSR regulon in *Staphylococcus aureus*. Antimicrob Agents Chemother 57:83–95 . doi: 10.1128/AAC.01651-12

Brown S, Santa Maria JP, Walker S, Walker S (2013) Wall teichoic acids of gram-positive bacteria. Annu Rev Microbiol 67:313–36 . doi: 10.1146/annurev-micro-092412-155620

Caboche S, Even G, Loywick A, Audebert C, Hot D (2017) MICRA: an automatic pipeline for fast characterization of microbial genomes from high-throughput sequencing data. Genome Biol 18:233 . doi: 10.1186/s13059-017-1367-z

Chang Y, Shin H, Lee J-H, Park CJ, Paik S-Y, Ryu S (2015) Isolation and genome characterization of the virulent *Staphylococcus aureus* bacteriophage SA97. Viruses 7:5225–5242 . doi: 10.3390/v7102870

Chaudhry WN, Concepcion-Acevedo J, Park T, Andleeb S, Bull JJ, Levin BR (2017) Synergy and order effects of antibiotics and phages in killing *Pseudomonas aeruginosa* biofilms. PLoS One 12:1–16 . doi: 10.1371/journal.pone.0168615

CLSI (2012) Methods for dilution antimicrobial susceptibility tests for bacteria that grow aerobically; approved standard- ninth edition. Clinical and Laboratory Standards Institute, Wayne, PA

Cui Z, Guo X, Dong K, Zhang Y, Li Q, Zhu Y, Zeng L, Tang R, Li L (2017) Safety assessment of *Staphylococcus* phages of the family Myoviridae based on complete genome sequences. Sci Rep 7:1–8 . doi: 10.1038/srep41259

Cumby N, Reimer K, Mengin-Lecreulx D, Davidson AR, Maxwell KL (2015) The phage tail tape measure protein, an inner membrane protein and a periplasmic chaperone play connected roles in the genome injection process of *E . coli* phage HK97. Mol Microbiol 96:437–447 . doi: 10.1111/mmi.12918

Doulgeraki AI, Di Ciccio P, Ianieri A, Nychas G-JE (2017) Methicillin-resistant food-related *Staphylococcus aureus*: a review of current knowledge and biofilm formation for future studies and applications. Res Microbiol 168:1–15 . doi: 10.1016/j.resmic.2016.08.001

Enright MC, Robinson DA, Randle G, Feil EJ, Grundmann H, Spratt BG (2002) The evolutionary history of methicillin-resistant *Staphylococcus aureus* (MRSA). Proc Natl Acad Sci U S A 99:7687–7692 . doi: 10.1073/pnas.122108599

Entenza M, Moreillon P, Guignard B (2005) b -lactams against methicillin-resistant

Staphylococcus aureus. Curr Opin Pharmacol 5:479–489 . doi: 10.1016/j.coph.2005.06.002

Espedido BA, Gosbell LB (2012) Chromosomal mutations involved in antibiotic resistance in Staphylococcus aures. Front Biosci 1:900–915

Fernandes S, São-José C (2018) Enzymes and mechanisms employed by tailed bacteriophages to breach the bacterial cell barriers. Viruses 10:396 . doi: 10.3390/v10080396

Foster TJ (2017) Antibiotic resistance in *Staphylococcus aureus*. Current status and future prospects. FEMS Microbiol Rev 41:430–449 . doi: 10.1093/femsre/fux007

Gerlach D, Guo Y, De Castro C, Kim S-H, Schlatterer K, Xu F-F, Pereira C, Seeberger PH, Ali S, Codée J, Sirisarn W, Schulte B, Wolz C, Larsen J, Molinaro A, Lee BL, Xia G, Stehle T, Peschel A (2018) Methicillin-resistant *Staphylococcus aureus* alters cell wall glycosylation to evade immunity. Nature 563:705–709 . doi: 10.1038/s41586-018-0730-x

Gnanamani A, Hariharan P, Paul-Satyaseela M (2017) *Staphylococcus aureus*: Overview of Bacteriology, Clinical Diseases, Epidemiology, Antibiotic Resistance and Therapeutic Approach. In: Frontiers in *Staphylococcus aureus*. InTech, pp 3–28

Gordillo Altamirano FL, Barr JJ (2019) Phage therapy in the postantibiotic era. Clin Microbiol Rev 32:1–25 . doi: 10.1128/cmr.00066-18

Goto H, Iwasaki M (2015) Susceptibilities of bacteria isolated from patients with lower respiratory infectious diseases to antibacterial agents (2008). Jpn J Antibiot 68:19–36

Haaber J, Penadés JR, Ingmer H, If TD, Penadés JR, Ingmer H, If TD (2017) Transfer of Antibiotic Resistance in *Staphylococcus aureus*. Trends Microbiol 25:893–905 . doi: 10.1016/j.tim.2017.05.011

Harada D, Nakaminami H, Miyajima E, Sugiyama T, Sasai N, Kitamura Y, Tamura T, Kawakubo T, Noguchi N (2018) Change in genotype of methicillin-resistant *Staphylococcus aureus* (MRSA) affects the antibiogram of hospital-acquired MRSA. J Infect Chemother 24:563–569 . doi: 10.1016/J.JIAC.2018.03.004

Hu B, Margolin W, Molineux IJ, Liu J (2015) Structural remodeling of bacteriophage T4 and host membranes during infection initiation. Proc Natl Acad Sci 112:E4919–E4928 . doi: 10.1073/pnas.1501064112

Hyman P, Abedon ST (2010) Bacteriophage host range and bacterial resistance. In: Allen IL, Sima S, Geoffrey MG (eds) Advances in applied microbiology, 1st edn. Elsevier Inc., Oxford, UK, pp 217–248

ICTV (2019) International Committee on Taxonomy of Viruses (ICTV). https://talk.ictvonline.org/taxonomy/. Accessed 5 Jun 2019

Kamal RM, Bayoumi MA, Abd El Aal SFA (2013) MRSA detection in raw milk, some dairy products and hands of dairy workers in Egypt, a mini-survey. Food Control 33:49–53 . doi: 10.1016/J.FOODCONT.2013.02.017

Klumpp J, Lavigne R, Loessner MJ, Ackermann H-W (2010) The SPO1-related bacteriophages. Arch Virol 155:1547–1561 . doi: 10.1007/s00705-010-0783-0

Kong K-F, Schneper L, Mathee K (2010) Beta-lactam antibiotics: from antibiosis to resistance and bacteriology. APMIS 118:1–36 . doi: 10.1111/j.1600-0463.2009.02563.x

Kumaran D, Taha M, Yi Q, Ramirez-Arcos S, Diallo J-S, Carli A, Abdelbary H (2018) Does treatment order matter? investigating the ability of bacteriophage to augment antibiotic activity against *Staphylococcus aureus* biofilms. Front Microbiol 9:127 . doi: 10.3389/fmicb.2018.00127

Kunishima H, Yamamoto N, Kaku M, Kunishima H, Kobayashi T, Minegishi M, Nakajima S, Chiba J, Kitagawa M, Honda Y, Hirakata Y (2010) Methicillin resistant *Staphylococcus aureus* in a Japanese community hospital: 5-year experience. J Infect Chemother 16:414–417 . doi: 10.1007/S10156-010-0076-2

Kurokawa K, Jung D-J, An J-H, Fuchs K, Jeon Y-J, Kim N-H, Li X, Tateishi K, Park JA, Xia G, Matsushita M, Takahashi K, Park H-J, Peschel A, Lee BL (2013) Glycoepitopes of staphylococcal wall teichoic acid govern complement-mediated opsonophagocytosis via human serum antibody and mannose-binding lectin. J Biol Chem 288:30956–30968 . doi: 10.1074/jbc.M113.509893

Kutter E (2009) Phage host range and efficiency of plating. In: Clokie MR, Kropinski AM (eds) Bacteriophages. Humana Press, New York, USA, pp 141–149

Lee AS, de Lencastre H, Garau J, Kluytmans J, Malhotra-Kumar S, Peschel A, Harbarth S (2018)

Methicillin resistance in *Staphylococcus aureus*. Nat Rev Dis Prim 4:18033 . doi: 10.1016/B978-0-12-813547-1.00017-0

Lee N. (2013) General nucleic acid extraction protocol. http://mibio.wzw.tum.de/. Accessed 6 Jun 2019

Lenhard JR, Eiff C Von, Hong IS, Holden PN, Bear MD, Suen A, Bulman ZP (2015) Evolution of *Staphylococcus aureus* under Vancomycin Selective Pressure : the Role of the Small-Colony Variant Phenotype. 59:1347–1351 . doi: 10.1128/AAC.04508-14

Leone S, Lauria FN, Nicastri E, Wenzel RP (2010) Methicillin-resistant *Staphylococcus aureus*: the superbug. Int J Infect Dis 14:S7–S11 . doi: 10.1016/J.IJID.2010.05.003

Li H (2013) Aligning sequence reads, clone sequences and assembly contigs with BWA-MEM. arXiv:13033997 00:1–3

Li H, Handsaker B, Wysoker A, Fennell T, Ruan J, Homer N, Marth G, Abecasis G, Durbin R (2009) The sequence alignment/map format and SAMtools. Bioinformatics 25:2078–2079 . doi: 10.1093/bioinformatics/btp352

Lin DM, Koskella B, Lin HC (2017) Phage therapy: an alternative to antibiotics in the age of multi-drug resistance. World J Gastrointest Pharmacol Ther 8:162 . doi: 10.4292/wjgpt.v8.i3.162

Loskill P, Pereira PM, Jung P, Bischoff M, Herrmann M, Pinho MG, Jacobs K (2014) Reduction of the peptidoglycan crosslinking causes a decrease in stiffness of the *Staphylococcus aureus* cell envelope. Biophys J 107:1082–1089 . doi: 10.1016/j.bpj.2014.07.029

Maeda T, Saga T, Miyazaki T, Kouyama Y, Harada S, Iwata M, Yoshizawa S, Kimura S, Ishii Y, Urita Y, Sugimoto M, Yamaguchi K, Tateda K (2012) Genotyping of skin and soft tissue infection (SSTI)-associated methicillin-resistant *Staphylococcus aureus* (MRSA) strains among outpatients in a teaching hospital in Japan: application of a phage-open reading frame typing (POT) kit. J Infect Chemother 18:906–914 . doi: 10.1007/s10156-012-0506-4

Mirzaei MK, Nilsson AS (2015) Isolation of phages for phage therapy: a comparison of spot tests and efficiency of plating analyses for determination of host range and efficacy. PLoS One 10:1–13 . doi: 10.1371/journal.pone.0118557

Moak M, Molineux IJ (2000) Role of the Gp16 lytic transglycosylase motif in bacteriophage T7 virions at the initiation of infection. Mol Microbiol 37:345–55

Moak M, Molineux IJ (2004) Peptidoglycan hydrolytic activities associated with bacteriophage virions. Mol Microbiol 51:1169–1183 . doi: 10.1046/j.1365-2958.2003.03894.x

Moelling K, Broecker F, Willy C, Moelling K, Broecker F, Willy C (2018) A wake-up call : we need phage therapy now. Viruses 10:1–14 . doi: 10.3390/v10120688

Moran GJ, Krishnadasan A, Gorwitz RJ, Fosheim GE, McDougal LK, Carey RB, Talan DA, EMERGEncy ID Net Study Group (2006) Methicillin-resistant *S. aureus* infections among patients in the emergency department. N Engl J Med 355:666–674 . doi: 10.1056/NEJMoa055356

Myers EW, Miller W (1988) Optimal alignments in linear space. Comput Appl Biosci 4:7–11

Nair D, Memmi G, Hernandez D, Bard J, Beaume M, Gill S, Francois P, Cheung AL (2011) Whole-genome sequencing of *Staphylococcus aureus* strain RN4220, a key laboratory strain used in virulence research, identifies mutations that affect not only virulence factors but also the fitness of the strain. J Bacteriol 193:2332–2335 . doi: 10.1128/JB.00027-11

Nobrega FL, Vlot M, Jonge PA, Dreesens LL, Beaumont HJE, Lavigne R, Dutilh BE, Brouns SJJ (2018) Targeting mechanisms of tailed bacteriophages. Nat Rev Microbiol. doi: 10.1038/s41579-018-0070-8

Ohtsubo Y, Ikeda-Ohtsubo W, Nagata Y, Tsuda M (2008) GenomeMatcher: A graphical user interface for DNA sequence comparison. BMC Bioinformatics 9:376 . doi: 10.1186/1471-2105-9-376

Örmälä A-M, Jalasvuori M (2013) Phage therapy. Bacteriophage 3:e24219 . doi: 10.4161/bact.24219

Osada K, Takeuchi I, Miyanaga K, Tanji Y (2017) Coevolution between *Staphylococcus aureus* isolated from mastitic milk and its lytic bacteriophage φSA012 in batch co-culture with serial transfer. Biochem Eng J 126:16–23 . doi: 10.1016/j.bej.2017.06.022

Paharik AE, Horswill AR (2016) The staphylococcal biofilm: adhesins, regulation, and host response. Microbiol Spectr 4:VMBF-0022-2015 . doi: 10.1128/microbiolspec.VMBF-0022-

2015

Papadopoulos P, Papadopoulos T, Angelidis AS, Boukouvala E, Zdragas A, Papa A, Hadjichristodoulou C, Sergelidis D (2018) Prevalence of *Staphylococcus aureus* and of methicillin-resistant *S. aureus* (MRSA) along the production chain of dairy products in north-western Greece. Food Microbiol 69:43–50 . doi: 10.1016/J.FM.2017.07.016

Percy MG, Gründling A (2014) Lipoteichoic Acid Synthesis and Function in Gram-Positive Bacteria. Annu Rev Microbiol 68:81–100 . doi: 10.1146/annurev-micro-091213-112949

Pinho MG (2008) Mechanisms of β-lactam and glycopeptide resistance in *Staphylococcus aureus*. In: Lindsay JA (ed) *Staphylococcus aureus*: molecular genetics. Caister academic press, Norfolk, UK, p 207

Pires DP, Oliveira H, Melo LDR, Sillankorva S, Azeredo J (2016) Bacteriophage-encoded depolymerases: their diversity and biotechnological applications. Appl Microbiol Biotechnol 100:2141–2151 . doi: 10.1007/s00253-015-7247-0

Piuri M, Hatfull GF (2006) A peptidoglycan hydrolase motif within the mycobacteriophage TM4 tape measure protein promotes efficient infection of stationary phase cells. Mol Microbiol 62:1569–85 . doi: 10.1111/j.1365-2958.2006.05473.x

Rahman MM, Hunter HN, Prova S, Verma V, Qamar A, Golemi-Kotra D (2016) The *Staphylococcus aureus* methicillin resistance factor FmtA is a D-amino esterase that acts on teichoic acids. MBio 7:1–11 . doi: 10.1128/mBio.02070-15

Rice P, Longden I, Bleasby A (2000) EMBOSS: The European Molecular Biology Open Software Suite. Trends Genet 16:276–277 . doi: 10.1016/S0168-9525(00)02024-2

Roberts GA, Houston PJ, White JH, Chen K, Stephanou AS, Cooper LP, Dryden DTF, Lindsay JA (2013) Impact of target site distribution for Type I restriction enzymes on the evolution of methicillin-resistant *Staphylococcus aureus* (MRSA) populations. Nucleic Acids Res 41:7472–7484 . doi: 10.1093/nar/gkt535

Rodríguez-Rubio L, Quiles-Puchalt N, Martínez B, Rodríguez A, Penadés JR, García P (2013) The peptidoglycan hydrolase of *Staphylococcus aureus* bacteriophage 11 plays a structural role in the viral particle. Appl Environ Microbiol 79:6187–90 . doi: 10.1128/AEM.01388-13

Schenk MF, de Visser JAG (2013) Predicting the evolution of antibiotic resistance. BMC Biol 11:14 . doi: 10.1186/1741-7007-11-14

Sharma S, Chatterjee S, Datta S, Prasad R, Dubey D, Prasad RK, Vairale MG (2017) Bacteriophages and its applications: an overview. Folia Microbiol (Praha) 62:17–55 . doi: 10.1007/s12223-016-0471-x

Shigemura K, Tanaka K, Okada H, Nakano Y, Kinoshita S, Gotoh A, Arakawa S, Fujisawa M (2005) Pathogen occurrence and antimicrobial susceptibility of urinary tract infection cases during a 20-year period (1983-2002) at a single institution in Japan. Jpn J Infect Dis 58:303–308

Silva JB, Storms Z, Sauvageau D (2016) Host receptors for bacteriophage adsorption. FEMS Microbiol Lett 363:fnw002 . doi: 10.1093/femsle/fnw002

Söding J, Biegert A, Lupas AN (2005) The HHpred interactive server for protein homology detection and structure prediction. Nucleic Acids Res 33:W244-248 . doi: 10.1093/nar/gki408

Suzuki M, Matsumoto M, Takahashi M, Hayakawa Y, Minagawa H (2009a) Identification of the clonal complexes of *Staphylococcus aureus* strains by determination of the conservation patterns of small genomic islets. J Appl Microbiol 107:1367–1374 . doi: 10.1111/j.1365-2672.2009.04321.x

Suzuki M, Tawada Y, Kato M, Hori H, Mamiya N, Hayashi Y, Nakano M, Fukushima R, Katai A, Tanaka T, Hata M, Matsumoto M, Takahashi M, Sakae K (2009b) Development of a rapid strain differentiation method for methicillin-resistant *Staphylococcus aureus* isolated in Japan by detecting phage-derived open-reading frames. Jpn J Infect Dis 62:386–389 . doi: 10.1111/j.1365-2672.2006.02932.x

Swoboda JG, Campbell J, Meredith TC, Walker S (2010) Wall teichoic acid function, biosynthesis, and inhibition. Chembiochem 11:35–45 . doi: 10.1002/cbic.200900557

Synnott AJ, Kuang Y, Kurimoto M, Yamamichi K, Iwano H, Tanji Y (2009) Isolation from sewage influent and characterization of novel *Staphylococcus aureus* bacteriophages with wide host ranges and potent lytic capabilities. Appl Environ Microbiol 75:4483–4490 . doi: 10.1128/AEM.02641-08

Tagliaferri TL, Jansen M, Horz H-P (2019) Fighting pathogenic bacteria on two fronts: phages and antibiotics as combined strategy. Front Cell Infect Microbiol 9:1–13 . doi: 10.3389/fcimb.2019.00022

Takeuchi I, Osada K, Azam AH, Asakawa H, Miyanaga K, Tanji Y (2016) The presence of two receptor-binding proteins contributes to the wide host range of staphylococcal twort-like phages. Appl Environ Microbiol 82:5763–5774 . doi: 10.1128/AEM.01385-16

Tang SS, Apisarnthanarak A, Hsu LY (2014) Mechanisms of β-lactam antimicrobial resistance and epidemiology of major community- and healthcare-associated multidrug-resistant bacteria. Adv Drug Deliv Rev 78:3–13 . doi: 10.1016/j.addr.2014.08.003

Toprak E, Veres A, Michel J-B, Chait R, Hartl DL, Kishony R (2011) Evolutionary paths to antibiotic resistance under dynamically sustained drug selection. Nat Genet 44:101–105 . doi: 10.1038/ng.1034

Torres-Barcel C, Hochberg ME (2016) Evolutionary rationale for phages as complements of antibiotics. Trends Microbiol 24:249–256 . doi: 10.1016/j.tim.2015.12.011

Uchiyama J, Takemura-Uchiyama I, Kato S-I, Sato M, Ujihara T, Matsui H, Hanaki H, Daibata M, Matsuzaki S (2014a) In silico analysis of AHJD-like viruses, *Staphylococcus aureus* phages S24-1 and S13', and study of phage S24-1 adsorption. Microbiologyopen 3:257–270 . doi: 10.1002/mbo3.166

Uchiyama J, Takemura-UchiyAma I, Kato SI, Sato M, Ujihara T, Matsui H, Hanaki H, Daibata M, Matsuzaki S (2014b) In silico analysis of AHJD-like viruses, *Staphylococcus aureus* phages S24-1 and S13', and study of phage S24-1 adsorption. Microbiologyopen 3:257–270 . doi: 10.1002/mbo3.166

Ung P, Peng C, Yuk S, Ann V, Mith H, Tan R, Miyanaga K, Tanji Y (2018) Fate of Escherichia coli in dialysis device exposed into sewage influent and activated sludge. J Water Health 16:380–390 . doi: 10.2166/hydro.2018.094

Vandersteegen K, Kropinski AM, Nash JHE, Noben J, Hermans K, Lavigne R (2013) Romulus and Remus , two phage isolates representing a distinct clade within the twortlikevirus genus , display suitable properties for phage therapy applications. J Virol 87:3237–3247 . doi: 10.1128/JVI.02763-12

Vollmer W, Blanot D, De Pedro MA, Scheffers D, Pinho M, Nikolaidis I, Favini-Stabile S, Dessen A, Matteï PJ, Neves D, Dessen A, Macheboeuf P, Lemaire D, Martins ADS, Dideberg O, Jamin M, Dessen A, Di Guilmi AM, Job V, Vernet T, Dideberg O, Dessen A, Contreras-Martel C, Job V, Dideberg O, Dessen A, Fischer DS, Brown Jr T, Zervosen A, Luxen A, Joris B, Dessen A, Schofield CJ, Holtje J V, Contreras-Martel C, Amoroso A, Woon EC, Zervosen A, Inglis S, Martins ADS, Verlaine O, Rydzik a M, Job V, Luxen A, Joris B, Schofield CJ, Dessen A (2005) Bacterial cell wall synthesis: new insights from localization studies. FEMS Microbiol Rev 30:565–569 . doi: 10.1128/MMBR.69.4.585

Walker BJ, Abeel T, Shea T, Priest M, Abouelliel A, Sakthikumar S, Cuomo CA, Zeng Q, Wortman J, Young SK, Earl AM (2014) Pilon: an integrated tool for comprehensive microbial variant detection and genome assembly improvement. PLoS One 9:e112963 . doi: 10.1371/journal.pone.0112963

Weidenmaier C, Peschel A (2008) Teichoic acids and related cell-wall glycopolymers in Gram-positive physiology and host interactions. Nat Rev Microbiol 6:276–287 . doi: 10.1038/nrmicro1861

WHO (2019) Ten threats to global health in 2019. https://www.who.int/emergencies/ten-threats-to-global-health-in-2019. Accessed 23 Feb 2019

WHO (2014) Antimicrobial resistance: global report on surveillance. Geneva

Winstel V, Xia G, Peschel A (2014) Pathways and roles of wall teichoic acid glycosylation in *Staphylococcus aureus*. Int J Med Microbiol 304:215–221 . doi: 10.1016/j.ijmm.2013.10.009

Xia G, Corrigan RM, Winstel V, Goerke C, Gründling A, Peschel A (2011) Wall teichoic acid-dependent adsorption of staphylococcal siphovirus and myovirus. J Bacteriol 193:4006–4009 . doi: 10.1128/JB.01412-10

Xia G, Kohler T, Peschel A (2010) The wall teichoic acid and lipoteichoic acid polymers of *Staphylococcus aureus*. Int J Med Microbiol 300:148–154 . doi: 10.1016/j.ijmm.2009.10.001

Xia G, Wolz C (2014) Phages of *Staphylococcus aureus* and their impact on host evolution. Infect Genet Evol 21:593–601 . doi: 10.1016/J.MEEGID.2013.04.022

Xiang Y, Morais MC, Cohen DN, Bowman VD, Anderson DL, Rossmann MG (2008) Crystal

and cryoEM structural studies of a cell wall degrading enzyme in the bacteriophage 29 tail. Proc Natl Acad Sci 105:9552–9557 . doi: 10.1073/pnas.0803787105

Zerbino DR, Birney E (2008) Velvet: algorithms for de novo short read assembly using de Bruijn graphs. Genome Res 18:821–829 . doi: 10.1101/gr.074492.107

Acknowledgement

First, I am grateful to my supervisor, prof. Yasunori TANJI, for his guidance, support, and help throughout my research.

I also would like to thank assistant prof. Kazuhiko MIYANAGA and Dr. Aa Haeruman AZAM, for giving me advice and facilitating my experiment. I am also thankful to prof. Tomoko HANAWA and her colleagues of Kyorin University Hospital for handling experiment with MRSA strains and allowing me to conduct the experiment in her laboratory.

I am very appreciated to Science and Technology Research Partnership for Sustainable Development (SATREPS), the Japan Science and Technology Agency (JST)/Japan International Cooperation Agency (JICA) with the grant-number JPMJSA1503, and the ASEAN University Network-Southeast Asia Engineering Education Development Network (AUN/SEED- Net) for funding my research and stay in Japan.

Last but not least, my deepest appreciation goes to my father and my husband for their motivation and encouragement. And special thanks to all of Tanji's laboratory members for their discussions during weekly lab seminar.

Journal Publication

1. Peng, C., Hanawa, T., Azam, AH., LeBlanc, C., Ung, P., Matsuda, T., Onishi, H., Miyanaga, K., Yasunori Tanji., Y. (2019). *Silviavirus* phage ϕMR003 displays a broad host range against methicillin-resistant *Staphylococcus aureus* of human origin. Applied Microbiology and Biotechnology. https://doi.org/10.1007/s00253-019-10039-2
2. Ung, P., Peng, C., Yuk, S., Tan, R., Ann, V., Miyanaga, K., Tanji, Y. (2019). Dynamics of bacterial community in Tonle Sap Lake, a large tropical flood-pulse system in Southeast Asia. Science of the Total Environment, 664, 414-423
3. Ung, P., Peng, C., Yuk, S., Ann, V., Mith, H., Tan, R., Miyanaga, K., Tanji, Y. (2018). Fate of *Escherichia coli* in dialysis device exposed into sewage influent and activated sludge. Journal of Water and Health,16 (3), 380-390